Stem Cell Reports

Derivation of brain capillary-like endothelial cells from human pluripotent stem cell-derived endothelial progenitor cells
--Manuscript Draft--

Manuscript Number:	STEM-CELL-REPORTS-D-18-00459R4
Article Type:	Report
Keywords:	Blood-brain barrier; iPSCs; brain capillary endothelial cells; soluble factors; extracellular matrices.
Corresponding Author:	lino ferreira University of Coimbra, Center of Neurosciences and Cell Biology Coimbra, PORTUGAL
First Author:	Catarina Praça
Order of Authors:	Catarina Praça
	Susana C Rosa
	Emmanuel Sevin
	Romeo Cecchelli
	Marie-Pierre Dehouck
	Lino Ferreira
Abstract:	The derivation of human brain capillary endothelial cells is of utmost importance for drug discovery programs focusing on diseases of the central nervous system. Here, we describe a two-step differentiation protocol to derive brain capillary-like endothelial cells from human pluripotent stem cells. The cells were initially differentiated into endothelial progenitor cells followed by specification into a brain capillary-like endothelial cell phenotype using a protocol that combined the induction, in a time-dependent manner, of VEGF, Wnt3a and RA signaling pathways and the use of fibronectin as the extracellular matrix. The brain capillary-like endothelial cells displayed a permeability to Lucifer yellow of 1×10^{-3} cm/min, a transendothelial electrical resistance value of 60 cm2 and were able to generate a continuous monolayer of cells expressing ZO-1 and CLAUDIN-5 but moderate expression of P-glycoprotein. Further maturation of these cells required the coculture with pericytes. The study presented here opens a new approach for the study of soluble and non-soluble factors in the specification of endothelial progenitor cells into brain capillary-like endothelial cells.

CENTER FOR NEUROSCIENCE AND CELL BIOLOGY
UNIVERSITY OF COIMBRA, PORTUGAL

Derivation of brain capillary-like endothelial cells from human pluripotent stem cell-derived endothelial progenitor cells

Catarina Praça[a,c], Susana C. Rosa[b], Emmanuel Sevin[c], Romeo Cecchelli[c], Marie-Pierre Dehouck[c] and Lino S. Ferreira[b,d*]

[a]*Doctoral Programme in Experimental Biology and Biomedicine (PDBEB), University of Coimbra, Portugal CNC - Center for Neuroscience and Cell Biology, University of Coimbra, Portugal; Institute for Interdisciplinary Research (IIIUC), University of Coimbra, Portugal;*
[b]*Center for Neuroscience and Cell Biology, University of Coimbra, Portugal*
[c]*Faculté des Sciences Jean Perrin, Université d´Artois, Lens, France*
[d]*Institute for Interdisciplinary Research (IIIUC), University of Coimbra, Portugal*
*corresponding author: lino@uc-biotech.pt

Online Summary

In this article, Ferreira and colleagues describe a protocol for the derivation of brain capillary-like endothelial cells from hiPSCs under fully chemically defined medium and extracellular matrix in 2 steps. The protocol requires the modulation of 3 signaling pathways (VEGF, WNT3a and retinoic acid) and the use of fibronectin as a single extracellular matrix component.

HIGHLIGHTS

- Derivation of brain capillary-like endothelial cells from hiPSCs under fully chemically defined medium and extracellular matrix in 2 steps.
- The activation of VEGF, Wnt3a and RA signaling pathways, at specific times, are required for the specification of endothelial progenitor cells into brain capillary-like endothelial cells.
- Fibronectin seems a sufficient substrate for the specification of endothelial progenitor cells into brain capillary-like endothelial cells.

Derivation of brain capillary-like endothelial cells from human pluripotent stem cell-derived endothelial progenitor cells

Catarina Praça[a,c], Susana C. Rosa[b], Emmanuel Sevin[c], Romeo Cecchelli[c], Marie-Pierre Dehouck[c] and Lino S. Ferreira[b,d*]

*a*Doctoral Programme in Experimental Biology and Biomedicine (PDBEB), University of Coimbra, Portugal CNC - Center for Neuroscience and Cell Biology, University of Coimbra, Portugal; Institute for Interdisciplinary Research (IIIUC), University of Coimbra, Portugal;
*b*Center for Neuroscience and Cell Biology, University of Coimbra, Portugal
*c*Faculté des Sciences Jean Perrin, Université d´Artois, Lens, France
*d*Institute for Interdisciplinary Research (IIIUC), University of Coimbra, Portugal
*corresponding author: lino@uc-biotech.pt

SUMMARY

The derivation of human brain capillary endothelial cells is of utmost importance for drug discovery programs focusing on diseases of the central nervous system. Here, we describe a two-step differentiation protocol to derive brain capillary-like endothelial cells from human pluripotent stem cells. The cells were initially differentiated into endothelial progenitor cells followed by specification into a brain capillary-like endothelial cell phenotype using a protocol that combined the induction, in a time-dependent manner, of VEGF, Wnt3a and RA signaling pathways and the use of fibronectin as the extracellular matrix. The brain capillary-like endothelial cells displayed a permeability to Lucifer yellow of 1×10^{-3} cm/min, a transendothelial electrical resistance value of 60 Ωcm^2 and were able to generate a continuous monolayer of cells expressing ZO-1 and CLAUDIN-5 but moderate expression of P-glycoprotein. Further maturation of these cells required the coculture with pericytes. The study presented here opens a new approach for the study of soluble and non-soluble factors in the specification of endothelial progenitor cells into brain capillary-like endothelial cells.

KEYWORDS: Blood-brain barrier, iPSCs, brain capillary endothelial cells, soluble factors, extracellular matrices

INTRODUCTION

The blood-brain barrier (BBB) is a physical and metabolic barrier formed by a specialized network of brain capillary endothelial cells (BCECs) that together with pericytes, astrocytes, microglia, neurons and extracellular matrix (ECM) form the functional neurovascular unit (NVU). BCECs are characterized by their low permeability to drugs mostly due to the high expression of tight junctions as well as the molecular influx and efflux transporters that selectively regulate the flux of molecules through the BBB (Abbott et al., 2010; Cecchelli et al., 2007; Aday et al., 2016; Zhao et al., 2015). In addition, BCECs present low vesicle trafficking, resulting in low rates of transcytosis (Siegenthaler et al., 2013; Villaseñor et al., 2018)

Pluripotent stem cells are a promising source of cells for the derivation of large numbers of brain capillary-like endothelial cells (BCLECs) to study BBB function in homeostasis and disease such as, Alzheimer´s and Parkinson diseases. Up until now, BCLECs have been derived from induced pluripotent stem cells (iPSCs) based on differentiation protocols relying on non-defined media (i.e. containing serum) (Lippmann et al., 2014; Lippmann et al., 2012; Katt et al., 2016; Appelt-Menzel et al., 2017; Lim et al., 2017; Katt et al., 2018; Ribecco-Lutkiewicz et al., 2018) or chemical defined media (Hollmann et al., 2017) without the isolation of endothelial progenitor cells (EPCs). In these protocols, BCLECs have been selectively purified from a mixture of different cell populations, containing neural progenitor cells, by using selective media and ECM.

Unfortunately, the heterogeneity inherent to the system precludes the study of the molecular mechanisms governing the specification of iPSCs into BCLECs. Furthermore, the yield and the final phenotype of the obtained BCLECs was dependent on the original iPSC line used (Lippmann et al., 2012). During the preparation of this work, a protocol for the derivation of BCLECs using an intermediary EPC population and chemically defined media was reported (Qian et al., 2017). The protocol consisted of the differentiation of iPSCs into EPCs (characterized by the expression of VEGFR2 and CD31) followed by their specification into BCLECs by exposure to retinoic acid (RA). Yet, the role of other soluble and non-soluble signaling molecules on BCLEC specification, the cell kinetics during specification as well as the permeability properties of BCLEC monolayers to small molecules was not investigated.

Here we describe a method to derive BCLECs from iPSCs based on the initial differentiation of iPSCs into EPCs followed by their specification into BCLECs by modulating three different signaling pathways (VEGF, RA and WNT) and providing variable ECM substrates. We monitored the process by following the expression of BCEC markers by flow cytometry, immunocytochemistry and gene expression analyses. To assess the functional properties of the obtained BCLECs we evaluated the transendothelial electrical resistance (TEER), paracellular permeability, response to pro-inflammatory stimuli and transport of P-glycoprotein (PGP) ligands. The BCLECs reported here are immature in nature but open new opportunities for future BBB disease modelling and drug screening initiatives.

RESULTS

Characterization of EPCs. iPSCs were differentiated for 10 days in conditions that promoted mesoderm differentiation (Figure 1A). Then, EPCs were isolated by magnetic

activated cell sorting (MACS) and the expression of BEC markers was performed by flow cytometry (Figure 1B) and immunocytochemistry (Figure 1C). Approximately 91% of the sorted cells expressed CD31, 90% VEGFR2, 97% GLUT-1, 51% CLAUDIN-5, 58% OCCLUDIN, and the expression of PGP was not detected (Figure 1B). The obtained EPCs were able to uptake acetylated low-density-lipoprotein (acLDL) and expressed OCCLUDIN, CLAUDIN-5 and ZO-1 without colocalization with cell junctions, suggesting that these cells were not yet specified into BCLECs (Figure 1C).

Screening of soluble factors for the specification of EPCs into BCLECs. VEGF (Engelhardt and Liebner, 2014), WNT (Daneman et al., 2009; Liebner et al., 2008; Stenman et al., 2008; Zhou and Nathans, 2014; Wang et al., 2018) and RA (Lippmann et al., 2014; Qian et al., 2017; Mizee et al., 2013) signaling have been reported as important players in early phases of BBB development. To specify EPCs into BCLECs, we modulated the three above-mentioned signaling pathways in a temporal manner (Figure 2A) using concentrations (VEGF: 50 ng/mL (Ferreira et al., 2007); Wnt3a: 10 ng/mL (Cecchelli et al., 2014); RA: 10 μM (Lippmann et al., 2014)) previously reported by us and others. Importantly, EPCs (passage 1) expressed frizzled receptors (*FZD4*, *6* and *7*) (Figure S1A1) and the concentration of Wnt3a used was enough to increase mRNA transcripts of downstream players of the Wnt3a signaling pathway, namely *LEF1* and *APCDD1* (Lippmann et al., 2012; Liebner et al., 2008) (Figure S1A2). No significant differences were observed for *AXIN2*. EPCs were cultured for 4 passages onto fibronectin-coated dishes in BM supplemented, or not, with different factors and the expression of BCEC markers was monitored over time by flow cytometry and qRT-PCR. The selection of fibronectin was based on the fact that, during the early stages of angiogenesis, when the specification of ECs into BCECs starts, ECs express predominantly fibronectin receptors ($\alpha 4\beta 1$ and $\alpha 5\beta 1$ integrins) (Milner and Campbell,

2002; Wang and Milner, 2006). Since collagen IV and fibronectin proteins are both part of the NVU ECM, we also tested the use of a combined mix of these substrates but no improvement was seen (data not shown). The expression of EC markers was lower in cells cultured in BM or BM+Wnt3a (Figures 2B-2C) than in the remaining conditions, suggesting that these culture conditions were less efficient in maintaining the EC phenotype. Because non-ECs have a significant impact in the barrier properties of ECs (Figure S1B), CD31$^+$ cells were purified and cultured to confluency on Matrigel-coated transwell inserts for 6 days after which paracellular permeability to Lucifer yellow (LY) and TEER analyses were performed. The monolayer of purified cells cultured in BM media showed a relatively high permeability to LY ($3\pm0.6\times10^{-3}$ cm/min) (Figure 2D) and low TEER (ca. 22.3 ± 1.5 Ωcm^2) (Figure 2E). The supplementation of BM with individual factors reduced the permeability of the EC barrier to LY (VEGF: $1.8\pm0.3\times10^{-3}$ cm/min; Wnt3a: $1.6\pm0.1\times10^{-3}$ cm/min; RA: $2.4\pm0.3\times10^{-3}$ cm/min) (Figure 2D). Interestingly, the supplementation of BM with a combination of factors (protocol 5: BM supplemented with VEGF and Wnt3a; protocol 6: BM supplemented with VEGF, Wnt3a and RA) yielded a EC barrier with higher TEER values (BM+VEGF+Wnt3a: 50 ± 0.8 Ωcm^2; BM+VEGF+Wnt3a+RA: 55 ± 0.6 Ωcm^2) (Figure 2E) and lower paracellular permeability to LY (BM+VEGF+Wnt3a: $1.2\pm0.2\times10^{-3}$ cm/min; BM+VEGF+Wnt3a+RA: $1.2\pm0.1\times10^{-3}$ cm/min) than cells cultured with BM or BM supplemented with each factor alone (Figure 2D). Thus, our results showed that BM supplemented with both VEGF, Wnt3a and RA offered the best approach to differentiate EPCs into BCLECs and generate a monolayer of cells with the highest TEER values and lowest paracellular permeability to LY. This chemically defined media was selected for the remaining experiments.

Screening of ECM for the specification of EPCs into BCLECs. ECM is an important component for the maintenance of BBB integrity (Baeten and Akassoglou, 2011; del

Zoppo and Milner, 2006). To evaluate the role of ECM in the induction of a BCEC phenotype from EPCs, we obtained decellularized ECM from primary bovine pericytes, bovine brain capillary endothelial cells (bBCECs) and rat glial cells (Figure S2). We found that the best time to decellularize the cell monolayers was between day 8 and 12, based in a compromise between the amount of deposited ECM and time (data not shown). In these conditions, regardless of the cell type, we obtained a decellularized matrix consisting of 1.5 to 2 $\mu g/cm^2$ of collagen (Figure S2C) which is in line with the value described for decellularized matrix obtained from mesenchymal stem cells (Prewitz et al., 2013). In addition, the decellularized matrix had relatively low levels of sulfated glycosaminoglycan (sGAG) (0.11 $\mu g/cm^2$ for bBCECs; data not shown), again in accordance with other studies (Prewitz et al., 2013). To evaluate the stability of the decellularized ECM, the matrices were kept in culture media, 4°C or 37°C, for 4 days and our results showed that approximately 50% of the collagen content was maintained after 4 days, regardless of the temperature (Figure S2D). Taken together, our results showed that we could prepare decellularized ECM from cells of the NVU.

To evaluate the effect of decellularized ECM in the induction of BCEC phenotype from EPCs, CD31^{+} cells were cultured on top of decellularized ECMs or fibronectin (control) for 3 passages (ca. 12 days), both in BM or BM supplemented with VEGF, Wnt3a and RA (Figure 3A). CD31^{+} cells adhered to glial and bBCEC decellularized ECM; however, they did not adhere well to the decellularized ECM of pericytes and died after some time. Therefore, only cells cultured on fibronectin and decellularized glial or bBCEC ECMs were characterized by flow cytometry at passage 4. Cells cultured in the glial decellularized ECM presented a lower co-expression of CD31:ZO-1 and CD31:CLAUDIN-5 and a higher co-expression of CD31:PGP than the ones cultured on fibronectin (Figure S2E1). Co-localization results, combined with the expression of

BCEC markers (Figure S2E), suggested that cells cultured on glial decellularized ECM expressed BBB markers but they were not all $CD31^+$ cells. Cells cultured on decellularized bBCEC ECM significantly lost their endothelial phenotype (as evaluated by CD31 marker) and showed low co-expression of CD31:ZO-1, CD31:CLAUDIN-5 and CD31:PGP (Figure S2E). These studies were complemented by gene analyses for a set of ECM, ECs and BCEC genes (Table S1) (Lippmann et al., 2012; Cecchelli et al., 2014; Armulik et al., 2010). Gene clustering analyses showed that $CD31^+$ cells cultured on fibronectin and BM supplemented with VEGF, Wnt3a and RA were more related to BCECs derived from a coculture of endothelial cells (ECs) (differentiated from human hematopoietic progenitor cells) with pericytes, previously described by us (Coculture condition; see ref. (Cecchelli et al., 2014)) (Figure 3B). Similar results were obtained using high throughput-gene expression analyses by Fluidigm (Figure S2F). Therefore, the decellularized glial ECM did not improve significantly the BCEC phenotype as compared to fibronectin.

Next, we evaluated the functional properties of the BCLECs obtained at passage 5 after purification using the CD31 marker. BCLECs were cultured to confluence on transwell inserts for 6 days after which paracellular permeability to LY and TEER analyses were performed. Cells cultured onto the decellularized glial ECM and fibronectin, but not in bBCEC ECM, expressed VE-CADHERIN, CLAUDIN-5 and ZO-1 at cell borders, and showed intercellular communication (Figure 3C). No difference in paracellular permeability to LY was observed between cells cultured onto fibronectin or onto decellularized ECM from glial cells; however, cells cultured onto decellularized bBCEC ECM showed higher paracellular permeability than cells cultured in the other conditions (Figure 3D). On the other hand, cells cultured onto fibronectin had higher TEER values than the ones cultured in the other conditions (Figure 3E).

Overall, our results showed that from the three decellularized ECMs tested, only decellularized glial ECM showed promising results in terms of EC phenotype maintenance, induction of BCEC markers and paracellular permeability; however, the results were not significantly different from the ones obtained with fibronectin. Therefore, subsequent tests were performed with CD31$^+$ cells cultured on fibronectin-coated plates in BM supplemented with VEGF, Wnt3a and RA.

Specification of EPCs into BCLECs: effect of time and pluripotent stem cell line. The induction of BCLEC properties in CD31$^+$ cells cultured on fibronectin-coated plates in the presence of BM supplemented with VEGF, Wnt3a and RA was monitored by flow cytometry and compared with CD31$^+$ cells cultured in BM alone. Flow cytometry analyses were performed at passage 2 (approximately 8 days in culture) and 4 (approximately 16 days in culture) and the co-localization of the CD31 marker with ZO-1, CLAUDIN-5 or PGP was quantified. Our results showed that cells cultured in BM supplemented with VEGF, Wnt3a and RA have higher co-localization of CD31 with ZO-1 or CLAUDIN-5 (Figure 4A) and this was further confirmed by confocal microscopy analyses (Figure S3A). As expected, the expression of BCEC markers was higher than the one observed in initial EPCs (Figure 1B-1C) or ECs without a BBB phenotype (Figure S3B) and similar, for some markers, to BCECs (hCMEC/D3 cell line) (Figure S3C). Noteworthy, the co-localization between CD31 and ZO-1/CLAUDIN-5 increased during time even though the differentiated cells expressed very low levels of PGP. Interestingly, our results showed that the CD31$^-$ subpopulation also expressed BCEC markers likely indicating the presence of intermediate phenotypic stages in the cell population (Figure 4A).

We next tested whether our differentiation protocol could generate BCLECs using different human pluripotent stem cell lines, including the human embryonic stem cell

line NKX2-5$^{eGFP/W}$ (Elliott et al., 2011) and iPSCs cell line derived from a Hutchinson-Gilford Progeria Syndrome (HGPS) fibroblast (Nissan et al., 2012). Using both pluripotent cell lines we were able to reproduce the differentiation protocol ultimately obtaining BCLECs expressing endothelial and BCEC markers (Figure S3D and S3E).

Functional characterization of BCLECs. CD31$^+$ cells were cultured on fibronectin-coated plates in the presence of BM supplemented with VEGF, Wnt3a and RA for 4 passages. At passage 5, cells were again purified for CD31 marker and grown to confluence on transwell inserts for 6 days after which the monolayer was characterized by immunocytochemistry (Figure 4B). Cells expressed typical endothelial surface markers, such as CD31, VE-CADHERIN and TIE-2, as well as intracellular markers such as von WILLEBRAND FACTOR (vWF), and were able to uptake ac-LDL (Figure 4B). Moreover, the obtained cells expressed BCEC markers including the tight-junction proteins ZO-1, CLAUDIN-5, OCCLUDIN and GLUT-1 (Figure 4B). The transporter PGP was expressed at moderate levels (Figure 4B). Furthermore, at transcriptional level, the differentiated cells showed lower expression of plasmalemma vesicle-associated protein (*PVLAP*) and a higher expression of multiple BBB genes such as tight junctions (*CLDN1* and *ZO-1*), influx amino acid (*SLC16A1*), receptors [(e.g. insulin receptor (*INSR*), transferrin receptor (*TFRC*) and low density lipoprotein receptor-related protein (*LRP1*)] and key efflux transporters such as *ABCB1* and multidrug resistance protein (*ABCC1* and *ABCC5*) than cells differentiated in BM conditions (Figure 4C). Based on the gene and protein expression results, as well as the paracellular permeability and TEER results (Figures 2C and 2D), the differentiated cells were named as BCLECs.

BCLECs constitutively expressed intracellular adhesion molecule (ICAM)-1 and -2 and responded to inflammatory stimuli such as tumor necrosis factor alpha (TNF-α) (Figure 4D). ICAM-1 was up-regulated in BCLECs (Figure 4D) and HUVECs (control;

Figure S4A) exposed to TNF-α, likely mediated by the activation of the pleiotropic nuclear factor–kB (NF-kB) (Collins et al., 1995), while ICAM-2 was slightly down-regulated in BCLECs after TNF-α, according to what is observed in HUVECs (Figure S4A) and previous studies (McLaughlin et al., 1998), when compared to the basal expression. BCLECs had no measurable expression of VCAM-1 by flow cytometry (data not shown), in agreement with other studies (Halaidych et al., 2018).

Because the expression of PGP in BCLECs was moderate, we evaluated whether the coculture with other cells from NVU would affect its expression and activity. We assessed the PGP activity and expression in BCLECs, with or without coculture for 6 days with bovine pericytes. The expression of PGP was not statistically different in BCLECs cocultured with pericytes as compared to BCLECs cultured as a monoculture (Figure 4E). Our results further showed that the inhibition of the PGP by elacridar led to a significant increase in the accumulation of Rhodamine123 in BCLECs cocultured with pericytes, but not when they were absent (Figure 4F).

Overall, the BCLECs obtained using our protocol expressed BCEC markers at gene and protein levels, they responded to inflammatory stimuli such as TNF-α and they showed efflux transporter activity when further matured in coculture with pericytes.

DISCUSSION

In this study, we described the derivation of BCLECs from iPSCs using a two-step protocol. Initially, we derived EPCs from human iPSCs after which they were specified into a BCLEC phenotype by exposure to both soluble and insoluble cues. After screening several soluble and insoluble factors, we showed that EPCs cultured on fibronectin for 4 passages (ca. 15-20 days) in BM supplemented with Wnt3a, VEGF and RA had a high expression of endothelial markers (CD31, VE-CADHERIN, vWF),

organized tight junctions at cell-cell junctions (ZO-1, CLAUDIN-5, OCCLUDIN), expressed nutrient transporters (GLUT-1) and some of them (ca. 40% of the cells) expressed efflux pumps (PGP), had a TEER similar to other human BCECs (TEER of ca. 60 Ωcm^2) (Cecchelli et al., 2014), displayed a paracellular permeability of 1×10^{-3} cm/min to LY and, upon exposure to TNF-α, they upregulated adhesion molecules such as ICAM-1 and downregulated ICAM-2. Overall, the obtained ECs showed a BCLEC phenotype. The current approach to generate BCLECs under fully chemically defined medium and ECM is desirable since (i) it will be more reproducible than existing protocols based on the use of KO-serum replacement or Matrigel-based substrates and (ii) it can contribute to unravel the mechanism(s) governing the specification into BCLEC. Indeed, here we show that the addition of Wnt3a at later stages improved the barrier properties of the cells in monolayer (Figure S4B) while the use of a coculture with pericytes in the presence of soluble factors identified in the current study, did not improve the barrier properties (Figure S4C). Moreover, the current approach recapitulates the developmental stages of rodent embryonic BBB formation, i.e., formation of EPCs that respond to VEGF signaling, followed by the specification of these cells into BCECs by the modulation of WNT signaling among other signaling pathways (Engelhardt and Liebner, 2014). Further studies are necessary to investigate whether this developmental recapitulation is extensive to human BBB development.

Recent studies have shown the derivation of BCLECs from iPSCs using a heterogeneous population of cells during differentiation and in non-defined media (Lippmann et al., 2014; Lippmann et al., 2012; Katt et al., 2016; Appelt-Menzel et al., 2017; Lim et al., 2017; Katt et al., 2018; Ribecco-Lutkiewicz et al., 2018). The differentiation protocol yielded on average 11.6 BCLECs per input iPSC, characterized by the co-expression of CD31 and GLUT-1 markers. These cells co-expressed

CLAUDIN-5 (~100%), OCCLUDIN (~100%), GLUT-1 (~70%) and PGP (~70%) (Lippmann et al., 2014; Lippmann et al., 2012). Our differentiation protocol yielded on average 10 BCLECs per input iPSC and the obtained cells co-expressed CLAUDIN-5 (~90%), OCCLUDIN (~100%), GLUT-1 (~100%) and PGP (~40%). Although the focus of the current work was to investigate the involvement of soluble and non-soluble factors, as well as the dynamics in the generation of a BCLEC phenotype from EPCs, much more effort is warranted to create a mature and functional BBB model characterized by cell polarization (not investigated in the current work), a high TEER and PGP expression as observed in primary BCECs (Hartmann et al., 2007) and other iPSC-derived BBB models (Qian et al., 2017). One of the major differences between our model and the ones previously described are related with the TEER values. It is important to note that TEER measurements are influenced by several parameters, including the equipment, temperature, medium composition and the area of the well, and thus it is difficult the comparison of TEER values between models and laboratories (Deli et al., 2005; Srinivasan et al., 2015). Although the *in vivo* TEER is estimated to be between 1000 and 2000 Ωcm^2 in rat or frog brains (Crone and Olesen, 1982; Butt et al., 1990), the *in vivo* TEER in humans remains to be determined. Moreover, the high TEER observed by some iPSC-derived BCLECs (Lippmann et al., 2012; Qian et al., 2017) has been questioned recently by recent single cell RNA analyses which have demonstrated that the cells presenting high TEER might have a neuroectodermal epithelial cell phenotype and not a BCLEC phenotype (Lu et al., 2019). Future studies should investigate the effect of initial density of EPCs in the functional outcome of BCLECs, as this variable might play an important role in differentiation/maturation of BCLECs (Qian et al., 2017; Wilson et al., 2015). In addition, to achieve a physiological barrier model, the effect of decellularized matrices from NVU at the end of the specification process as well as the use of cocultures

with cells from NVU should be investigated. Indeed, our results indicate that the coculture of BCLECs with pericytes further mature the cells as confirmed by a higher activity of PGP and low expression of transcripts of transcytosis genes (*PVLAP* and *CAV-1*) (Daneman et al., 2010; Ben-Zvi et al., 2014) (Figure S4D) as compared to a monoculture of BCLECs.

The control of Wnt3a, VEGF and RA signaling pathways seems important for the specification of EPCs into BCLECs. Previous studies using iPSCs have shown that canonical Wnt-β-catenin (Lippmann et al., 2012) and RA (Lippmann et al., 2014; Katt et al., 2016) signaling was necessary for the specification of BBB properties in ECs. Our results further showed that the use of VEGF was important to maintain the endothelial phenotype during the specification of the cells.

ECM provides physical support and presents biomolecules that may be important for the BBB specification process (Katt et al., 2016; Daneman et al., 2010). Previous studies have demonstrated that ECM produced by cells forming the NVU (glial and pericytes) improved the barrier function of BCECs cultured *in vitro* (Hartmann et al., 2007). Others have evaluated the effect of artificial ECMs such as Matrigel´s in the differentiation of iPSCs into BCECs (Patel and Alahmad, 2016). The current study evaluates the effect of decellularized ECM from the NVU in the specification of iPSCs into BCLECs. Our results showed that EPCs were unable to adhere to pericyte decellularized ECM but they could attach to the decellularized matrix of bBCECs and glial cells. Cells differentiated on top of decellularized glial ECM showed the highest BCLEC phenotype after 4 passages, the highest TEER and the lowest paracellular permeability to LY. However, the results obtained were not significantly different from the ones obtained on fibronectin-coated dishes. We cannot discard the possibility that the decellularized ECM might play a role in the polarization of BCLECs, a topic that deserves

further investigation in the near future. Moreover, the decellularized matrices from NVU were obtained from animal sources (bovine pericytes, bBCECs and rat glial cells) due to availability reasons. Future studies should explore the impact of decellularized ECMs from human origin.

The work presented here may contribute for a better understanding of the processes underlying the BBB development and maintenance. BBB formation is initiated at embryonic day 12 in the rat cerebral cortex by ECs that invade the neural tissue from the surrounding vascular plexus (Daneman et al., 2010). BBB-forming ECs are characterized by the expression of tight junctions including OCCLUDIN, CLAUDIN-5 and ZO-1 and the influx transporter GLUT-1. Interestingly, these cells express low levels of PGP that only increase during postnatal development (Daneman et al., 2010). Our *in vitro* results recapitulate this process since moderate levels of PGP were observed in BCLECs. Previous studies have derived BCLECs with high expression of PGP which may indicate a high level of BBB maturation (Lippmann et al., 2012; Katt et al., 2016). In addition, our results showed that the specification of EPCs into BCLECs is a slow process given that the expression of ZO-1, CLAUDIN-5 and PGP increased in CD31^{+} cells over 4 passages. Because CD31^{-} cells also expressed BCEC markers, future studies should further characterize these cells as well as their importance in the formation of a BBB.

Overall, the methodology reported in this work opens an opportunity to study the effect of soluble and non-soluble factors in the specification of EPCs into BCLECs, the dynamics of BCEC markers expression and the functionality of the derived cells.

EXPERIMENTAL PROCEDURES

Details are provided in Supplemental Experimental Procedures.

Derivation of BCLECs. iPSCs cell lines generated from human cord blood (passages: 30-40; K2- iPSC line) (Haase et al., 2009) or from Hutchinson-Gilford Progeria Syndrome (HGPS) fibroblasts (passages: 43-51) (Nissan et al., 2012) were used in the present study and were provided by the laboratories in which they were derived. For some experiments, the human embryonic stem cell line NKX2-5[eGFP/W] (passages: 40-45) (Elliott et al., 2011) was used. To initiate the differentiation, iPSCs ($27 \times 10^3 - 45 \times 10^3$ cells per cm^2) were treated for 45-60 min with collagenase IV and plated on fibronectin-coated dishes (1 µg/cm^2; Calbiochem) in a chemically defined medium (CDM) (see supplemental information). During the 10 days of the differentiation several factors were added to CDM medium in order to induce the formation of EPCs (CD31$^+$ cells) (Rosa et al., 2019). CD31$^+$ cells were isolated by MACS (Miltenyi Biotec), plated on fibronectin-coated dishes (1 µg/cm^2) and cultured in EGM-2 (Lonza) supplemented with SB 431542 (10 µM, Tocris Biosciences), bFGF (1 ng/mL, Sigma) and VEGF$_{165}$ (50 ng/mL, PeproTech) for 1 passage. Cells were then cultured in BM (EGM-2 supplemented with 10 µM SB 431542 and 1 ng/mL bFGF) or BM supplemented with VEGF$_{165}$ (25 ng/mL), Wnt3a (10 ng/mL, R&D Systems) or RA (10 µM, Sigma), alone or in combination, for 3 passages (approximately 15-20 days; Figure 2A). In a separate set of experiments, CD31$^+$ cells were plated on fibronectin-coated dishes or in decellularized native ECMs from pericytes, glial cells and bBCECs in the presence of BM or BM supplemented with VEGF$_{165}$, Wnt3a and RA (Figure 3A). During the differentiation procedure, cells were passed systematically every 4 days, in a split ratio of 1:3. Cells plated in the transwell inserts were cultured in EGM-2 supplemented with bFGF (1 ng/mL).

Statistical Analyses. For analyses involving three or more groups, an ANOVA test was used, followed by a Dunnett's or Tukey's post-test. For analysis of two groups, unpaired *t*-test was used. Statistical analysis was performed using GraphPad Prism software.

Results were considered significant when $P \leq 0.05$. In case of results having 3 independent runs and 3 technical replicates per independent run, the statistics were performed based in the 9 values (not by the means of each experiment).

AUTHORS CONTRIBUTIONS

LF, CP and SR conceived the study. CP and SR performed cell culture and decellularization experiments, gene, flow cytometry, immunocytochemistry and TEER analyses. ES, RC and MPD performed PGP inhibition studies and contributed with neural cells. All authors contributed to manuscript preparation.

ACKNOWLEDGMENTS

REFERENCES

Abbott, N. J., Patabendige, A. A., Dolman, D. E., Yusof, S. R. and Begley, D. J. (2010). Structure and function of the blood-brain barrier. Neurobiol Dis *1*, 13-25.

Cecchelli, R., Berezowski, V., Lundquist, S., Culot, M., Renftel, M., Dehouck, M. P. and Fenart, L. (2007). Modelling of the blood-brain barrier in drug discovery and development. Nature reviews. Drug discovery *8*, 650-61.

Aday, S., Cecchelli, R., Hallier-Vanuxeem, D., Dehouck, M. P. and Ferreira, L. (2016). Stem Cell-Based Human Blood-Brain Barrier Models for Drug Discovery and Delivery. Trends Biotechnol *5*, 382-393.

Zhao, Z., Nelson, A. R., Betsholtz, C. and Zlokovic, B. V. (2015). Establishment and Dysfunction of the Blood-Brain Barrier. Cell *5*, 1064-1078.

Siegenthaler, J. A., Sohet, F. and Daneman, R. (2013). 'Sealing off the CNS': cellular and molecular regulation of blood-brain barriergenesis. Current opinion in neurobiology *6*, 1057-64.

Villaseñor, R., Lampe, J., Schwaninger, M. and Collin, L. (2018). Intracellular transport and regulation of transcytosis across the blood–brain barrier. Cellular and Molecular Life Sciences

Lippmann, E. S., Al-Ahmad, A., Azarin, S. M., Palecek, S. P. and Shusta, E. V. (2014). A retinoic acid-enhanced, multicellular human blood-brain barrier model derived from stem cell sources. Sci Rep 4160.

Lippmann, E. S., Azarin, S. M., Kay, J. E., Nessler, R. A., Wilson, H. K., Al-Ahmad, A., Palecek, S. P. and Shusta, E. V. (2012). Derivation of blood-brain barrier endothelial cells from human pluripotent stem cells. Nat Biotechnol *8*, 783-91.

Katt, M. E., Xu, Z. S., Gerecht, S. and Searson, P. C. (2016). Human Brain Microvascular Endothelial Cells Derived from the BC1 iPS Cell Line Exhibit a Blood-Brain Barrier Phenotype. PLoS One *4*, e0152105.

Appelt-Menzel, A., Cubukova, A., Gunther, K., Edenhofer, F., Piontek, J., Krause, G., Stuber, T., Walles, H., Neuhaus, W. and Metzger, M. (2017). Establishment of a Human Blood-Brain Barrier Co-culture Model Mimicking the Neurovascular Unit Using Induced Pluri- and Multipotent Stem Cells. Stem Cell Reports *4*, 894-906.

Lim, R. G., Quan, C., Reyes-Ortiz, A. M., Lutz, S. E., Kedaigle, A. J., Gipson, T. A., Wu, J., Vatine, G. D., Stocksdale, J., Casale, M. S., Svendsen, C. N., Fraenkel, E., Housman, D. E., Agalliu, D. and Thompson, L. M. (2017). Huntington's Disease iPSC-Derived Brain Microvascular Endothelial Cells Reveal WNT-Mediated Angiogenic and Blood-Brain Barrier Deficits. Cell Rep *7*, 1365-1377.

Katt, M. E., Linville, R. M., Mayo, L. N., Xu, Z. S. and Searson, P. C. (2018). Functional brain-specific microvessels from iPSC-derived human brain microvascular endothelial cells: the role of matrix composition on monolayer formation. Fluids Barriers CNS *1*, 7.

Ribecco-Lutkiewicz, M., Sodja, C., Haukenfrers, J., Haqqani, A. S., Ly, D., Zachar, P., Baumann, E., Ball, M., Huang, J., Rukhlova, M., Martina, M., Liu, Q., Stanimirovic, D., Jezierski, A. and Bani-Yaghoub, M. (2018). A novel human induced pluripotent stem cell blood-brain barrier model: Applicability to study antibody-triggered receptor-mediated transcytosis. Sci Rep *1*, 1873.

Hollmann, E. K., Bailey, A. K., Potharazu, A. V., Neely, M. D., Bowman, A. B. and Lippmann, E. S. (2017). Accelerated differentiation of human induced pluripotent stem cells to blood-brain barrier endothelial cells. Fluids Barriers CNS *1*, 9.

Qian, T., Maguire, S. E., Canfield, S. G., Bao, X., Olson, W. R., Shusta, E. V. and Palecek, S. P. (2017). Directed differentiation of human pluripotent stem cells to blood-brain barrier endothelial cells. Science advances *11*, e1701679.

Engelhardt, B. and Liebner, S. (2014). Novel insights into the development and maintenance of the blood-brain barrier. Cell and tissue research *3*, 687-99.

Daneman, R., Dritan Agalliu, D., Zhou, L., Kuhnert, F., Kuo, C. J. and Barres, B. A. (2009). Wnt/beta-catenin signaling is required for CNS, but not non-CNS, angiogenesis. PNAS 641-646.

Liebner, S., Corada, M., Bangsow, T., Babbage, J., Taddei, A., Czupalla, C. J., Reis, M., Felici, A., Wolburg, H., Fruttiger, M., Taketo, M. M., von Melchner, H., Plate, K. H., Gerhardt, H. and Dejana, E. (2008). Wnt/beta-catenin signaling controls development of the blood-brain barrier. J Cell Biol *3*, 409-417.

Stenman, J. M., Rajagopal, J., Carroll, T. J., Ishibashi, M., McMahon, J. and McMahon, A. P. (2008). Canonical Wnt signaling regulates organ-specific assembly and differentiation of CNS vasculature. Science *5905*, 1247-50.

Zhou, Y. and Nathans, J. (2014). Gpr124 controls CNS angiogenesis and blood-brain barrier integrity by promoting ligand-specific canonical wnt signaling. Developmental cell *2*, 248-56.

Wang, Y., Cho, C., Williams, J., Smallwood, P. M., Zhang, C., Junge, H. J. and Nathans, J. (2018). Interplay of the Norrin and Wnt7a/Wnt7b signaling systems in blood–brain barrier and blood–retina barrier development and maintenance. Proceedings of the National Academy of Sciences *50*, E11827-E11836.

Mizee, M. R., Wooldrik, D., Lakeman, K. A., van het Hof, B., Drexhage, J. A., Geerts, D., Bugiani, M., Aronica, E., Mebius, R. E., Prat, A., de Vries, H. E. and Reijerkerk, A. (2013). Retinoic acid induces blood-brain barrier development. J Neurosci *4*, 1660-71.

Ferreira, L. S., Gerecht, S., Shieh, H. F., Watson, N., Rupnick, M. A., Dallabrida, S. M., Vunjak-Novakovic, G. and Langer, R. (2007). Vascular progenitor cells isolated from human embryonic stem cells give rise to endothelial and smooth muscle like cells and form vascular networks in vivo. Circulation Research *3*, 286-94.

Cecchelli, R., Aday, S., Sevin, E., Almeida, C., Culot, M., Dehouck, L., Coisne, C., Engelhardt, B., Dehouck, M. P. and Ferreira, L. (2014). A stable and reproducible human blood-brain barrier model derived from hematopoietic stem cells. PLoS One *6*, e99733.

Milner, R. and Campbell, I. L. (2002). Developmental regulation of beta1 integrins during angiogenesis in the central nervous system. Molecular and cellular neurosciences *4*, 616-26.

Wang, J. and Milner, R. (2006). Fibronectin promotes brain capillary endothelial cell survival and proliferation through alpha5beta1 and alphavbeta3 integrins via MAP kinase signalling. Journal of neurochemistry *1*, 148-59.

Baeten, K. M. and Akassoglou, K. (2011). Extracellular matrix and matrix receptors in blood-brain barrier formation and stroke. Dev Neurobiol *11*, 1018-39.

del Zoppo, G. J. and Milner, R. (2006). Integrin-matrix interactions in the cerebral microvasculature. Arterioscler Thromb Vasc Biol *9*, 1966-75.

Prewitz, M. C., Seib, F. P., von Bonin, M., Friedrichs, J., Stissel, A., Niehage, C., Muller, K., Anastassiadis, K., Waskow, C., Hoflack, B., Bornhauser, M. and Werner, C. (2013). Tightly anchored tissue-mimetic matrices as instructive stem cell microenvironments. Nat Methods *8*, 788-+.

Armulik, A., Genove, G., Mae, M., Nisancioglu, M. H., Wallgard, E., Niaudet, C., He, L., Norlin, J., Lindblom, P., Strittmatter, K., Johansson, B. R. and Betsholtz, C. (2010). Pericytes regulate the blood-brain barrier. Nature *7323*, 557-61.

Elliott, D. A., Braam, S. R., Koutsis, K., Ng, E. S., Jenny, R., Lagerqvist, E. L., Biben, C., Hatzistavrou, T., Hirst, C. E., Yu, Q. C., Skelton, R. J., Ward-van Oostwaard, D., Lim, S. M., Khammy, O., Li, X., Hawes, S. M., Davis, R. P., Goulburn, A. L., Passier, R., Prall, O. W., Haynes, J. M., Pouton, C. W., Kaye, D. M., Mummery, C. L., Elefanty, A. G. and Stanley, E. G. (2011). NKX2-5(eGFP/w) hESCs for isolation of human cardiac progenitors and cardiomyocytes. Nat Methods *12*, 1037-40.

Nissan, X., Blondel, S., Navarro, C., Maury, Y., Denis, C., Girard, M., Martinat, C., De Sandre-Giovannoli, A., Levy, N. and Peschanski, M. (2012). Unique preservation of neural cells in Hutchinson- Gilford progeria syndrome is due to the expression of the neural-specific miR-9 microRNA. Cell Rep *1*, 1-9.

Collins, T., Read, M. A., Neish, A. S., Whitley, M. Z., Thanos, D. and Maniatis, T. (1995). Transcriptional regulation of endothelial cell adhesion molecules: NF-kappa B and cytokine-inducible enhancers. FASEB J *10*, 899-909.

McLaughlin, F., Hayes, B. P., Horgan, C. M., Beesley, J. E., Campbell, C. J. and Randi, A. M. (1998). Tumor necrosis factor (TNF)-alpha and interleukin (IL)-1beta down-regulate intercellular adhesion molecule (ICAM)-2 expression on the endothelium. Cell adhesion and communication *5*, 381-400.

Halaidych, O. V., Freund, C., van den Hil, F., Salvatori, D. C. F., Riminucci, M., Mummery, C. L. and Orlova, V. V. (2018). Inflammatory Responses and Barrier Function of Endothelial Cells Derived from Human Induced Pluripotent Stem Cells. Stem Cell Reports *5*, 1642-1656.

Hartmann, C., Zozulya, A., Wegener, J. and Galla, H.-J. (2007). The impact of glia-derived extracellular matrices on the barrier function of cerebral endothelial cells: An in vitro study. Experimental Cell Research *7*, 1318-1325.

Deli, M. A., Abraham, C. S., Kataoka, Y. and Niwa, M. (2005). Permeability studies on in vitro blood-brain barrier models: physiology, pathology, and pharmacology. Cellular and molecular neurobiology *1*, 59-127.

Srinivasan, B., Kolli, A. R., Esch, M. B., Abaci, H. E., Shuler, M. L. and Hickman, J. J. (2015). TEER measurement techniques for in vitro barrier model systems. Journal of laboratory automation *2*, 107-26.

Crone, C. and Olesen, S. P. (1982). Electrical resistance of brain microvascular endothelium. Brain Res *1*, 49-55.

Butt, A. M., Jones, H. C. and Abbott, N. J. (1990). Electrical resistance across the blood-brain barrier in anaesthetized rats: a developmental study. J Physiol 47-62.

Lu, T. M., Redmond, D., Magdeldin, T., Nguyen, D.-H. T., Snead, A., Sproul, A., Xiang, J., Shido, K., Fine, H. A., Rosenwaks, Z., Rafii, S., Agalliu, D. and Lis, R. (2019). Human induced pluripotent stem cell-derived neuroectodermal epithelial cells mistaken for blood-brain barrier-forming endothelial cells. bioRxiv. doi: http://dx.doi.org/10.1101/699173.

Wilson, H. K., Canfield, S. G., Hjortness, M. K., Palecek, S. P. and Shusta, E. V. (2015). Exploring the effects of cell seeding density on the differentiation of human pluripotent stem cells to brain microvascular endothelial cells. Fluids Barriers CNS 13.

Daneman, R., Zhou, L., Kebede, A. A. and Barres, B. A. (2010). Pericytes are required for blood-brain barrier integrity during embryogenesis. Nature *7323*, 562-6.

Ben-Zvi, A., Lacoste, B., Kur, E., Andreone, B. J., Mayshar, Y., Yan, H. and Gu, C. (2014). Mfsd2a is critical for the formation and function of the blood-brain barrier. Nature *7501*, 507-11.

Patel, R. and Alahmad, A. J. (2016). Growth-factor reduced Matrigel source influences stem cell derived brain microvascular endothelial cell barrier properties. Fluids Barriers CNS 6.

Haase, A., Olmer, R., Schwanke, K., Wunderlich, S., Merkert, S., Hess, C., Zweigerdt, R., Gruh, I., Meyer, J., Wagner, S., Maier, L. S., Han, D. W., Glage, S., Miller, K., Fischer, P., Schöler, H. R. and Martin, U. (2009). Generation of Induced Pluripotent Stem Cells from Human Cord Blood. Cell Stem Cell *4*, 434-441.

Rosa, S., Praca, C., Pitrez, P. R., Gouveia, P. J., Aranguren, X. L., Ricotti, L. and Ferreira, L. S. (2019). Functional characterization of iPSC-derived arterial- and venous-like endothelial cells. Sci Rep *1*, 3826.

FIGURE LEGENDS

Figure 1 – Characterization of EPCs. (A) Scheme of hiPSCs differentiation into BCLECs. hiPSCs were first differentiated during 10 days into EPCs (CD31$^+$ cells). These cells were then isolated by MACS and specified/expanded into BCLECs for 4 passages. **(B)** Expression of BCEC markers was assessed by flow cytometry on isolated CD31$^+$ cells. Percentages of positive cells were calculated based in the isotype controls (1%; dark blue scatter plot). **(C)** Expression of BCEC markers on CD31$^+$ cells by immunocytochemistry. Scale bar corresponds to 50 μm.

Figure 2 – Effect of soluble factors in the specification of EPCs into BCLECs. (A) Schematic representation of the protocols used to specify CD31$^+$ onto BCLECs. **(B)** Expression of CD31 marker on ECs at passage 4 was assessed by flow cytometry. Percentages of positive cells were calculated based in the isotype controls (1%; dark blue scatter plot). **(C)** Fold change of endothelial gene expression in ECs cultured in the different protocols at passage 4 (without purification) relative to ECs cultured in BM conditions. Genes were normalized against the control gene *β-ACTIN*. Values are Mean ± SEM (n=3 independent experiment, 3 technical replicates per experimental condition). *P<0.05, **P<0.01* and ****P<0.0001* using one-way ANOVA followed by Dunnett's

multiple comparison test. **(D)** Paracellular permeability to LY and **(E)** TEER in cells either exposed or not to the chemical factors with purification 6 days after being plated on Matrigel-coated transwell inserts. In D and E, hCMEC/D3 cell line and human hematopoietic progenitor cell-derived ECs cocultured with pericytes for 6 days (coculture condition) (Cecchelli et al., 2014) were used as controls. In D and E, values are Mean ± SEM (n=3 independent experiments; at least 3 transwell inserts per independent experiment and experimental condition). *P<0.05*, **P<0.01* and ***P<0.001* using one-way ANOVA followed by Dunnett's multiple comparison test. See also Figure S1.

Figure 3 - Effect of the combination of soluble factors with decelullarized ECMs in the specification of EPCs into BCLECs. (A) Schematic representation of the protocols used to maturate the CD31⁺ to BCLECs. Cells were cultured for 3 passages either on fibronectin (control) or on decellularized ECM and then purified and plated on Matrigel-coated transwell inserts for 6 days. **(B)** Relative gene expression levels on cells cultured on BM or BM+VEGF+Wnt3a+RA either on fibronectin or glial ECM (positive control was "coculture" condition, i.e., human hematopoietic stem/progenitor-derived ECs cocultured with pericytes, please see ref (Cecchelli et al., 2014) followed by their plating on Matrigel-coated transwell inserts for 6 days. Heatmap and hierarchical clustering dendogram are displayed. Genes were normalized against the control gene *β-ACTIN*. (n=1 independent experiment, 3 technical replicates per experimental condition). Relative gene expression is provided as Table S1. For each gene, the normalized values were between +0.5 and -0.5 (please see Supplementary Information for the detailed calculation procedure). Gene expression that was above the gene expression median for all the experimental groups was shown in red, the expression below the median in blue and the expression similar to the median in white. **(C)** Expression of CLAUDIN-5, ZO-1 and VE-CADHERIN in BCLECs plated on Matrigel-coated transwell inserts for 6 days. Scale bar

corresponds to 50 μm. **(D)** Paracellular permeability to LY and **(E)** TEER on cells specified in different ECMs and media followed by their purification and culture for 6 days on Matrigel-coated transwell inserts. In D and E, values are Mean ± SEM (n=3 independent experiments; at least 3 transwell inserts per independent experiment and experimental condition). **P<0.01* and ****P<0.0001* using one-way ANOVA followed by Tukey's multiple comparison test. See also Figure S2.

Figure 4 – Impact of time in the specification of EPCs into BCLECs and BCLECs functional characterization. (A) Expression by flow cytometry of BCEC markers (ZO-1, CLAUDIN-5 and PGP) co-localized with CD31 marker on cells specified in different inductive mediums (BM and BM+VEGF+Wnt3a+RA) at passage 2 and passage 4. Percentages of positive cells were calculated based in the isotype controls (1%). **(B)** Expression of BCEC markers on BCLECs by immunofluorescence after 6 days on Matrigel-coated transwell inserts. Scale bar corresponds to 50 μm. **(C)** Relative gene expression on cells plated on Matrigel-coated transwell inserts for 6 days after specification on BM or BM+VEGF+Wnt3a+RA. Values are Mean ± SEM (n=3 independent experiment, 3 technical replicates per experimental condition). *P<0.05* and ****P<0.001* using unpaired t-test. **(D)** Expression of adhesion molecules (ICAM-1 and ICAM-2) on BCLECs at basal level and after exposure to TNF-α (10 ng/mL) for 24 h. Percentage of positive cells was calculated based in the gates defined for the basal expression of the marker (1%; light blue). **(E)** Expression of PGP on BCLECs cultured alone or in coculture with pericytes for 6 days on Matrigel-coated transwell inserts. Percentage of positive cells was calculated based in the gates defined for the isotype control (1%; dark blue). Values are Mean ± SEM (n=3 independent experiments). No statistical difference was observed between means as evaluated by an unpaired t-test. **(F)** Accumulation of rhodamine 123 after inhibition of BCLECs cultured alone or in

coculture with pericytes for 6 days on Matrigel-coated transwell inserts with elacridar. Values are Mean ± SEM (n=3 independent experiments; 3 transwell inserts per independent experiment and experimental condition). **P<0.01* using unpaired t-test. See also Figures S3-S4.

Table S1 – Relative gene expression data for heatmap (in Excel format). The gene expression was normalized against the endogenous control *(β-ACTIN)* and presented as relative gene expression. The genes are in order by which they appeared in the heatmap. Related with Figure 3.

SUPPLEMENTAL INFORMATION

Supplemental Information includes Supplemental Experimental Procedures, 4 figures and 4 tables and can be found with this article online.

Figure 1

A 10 days Differentiation → CD31⁺ cells (EPCs) → 5 Passages (≈ 15-20 days) Expansion and differentiation into Brain capillary-like endothelial cells

B

CD31 FITC — 91%
VEGFR2 PE — 90%
GLUT-1 PE — 97%
OCCLUDIN PE — 58%
CLAUDIN-5 PE — 51%
PGP PE — 0%

C

CD31, TIE2, vWF, acLDL
GLUT-1, ZO-1, CLAUDIN-5, OCCLUDIN

Figure 2

A

Well plate (ca. 15-20 days)   Transwell (6 days)

P0   P1   P2   P5

1   BM + VEGF_50   BM
2   BM + VEGF_50   BM + VEGF
3   BM + VEGF_50   BM + Wnt3a
4   BM + VEGF_50   BM + RA   BM
5   BM + VEGF_50   BM + Wnt3a+ VEGF
6   BM + VEGF_50   BM + Wnt3a + VEGF + RA   BM + Wnt3a + VEGF

B

BM — 50%
BM+VEGF — 84%
BM+Wnt3a — 46%
BM+RA — 76%
BM+VEGF+Wnt3a — 75%
BM+VEGF+Wnt3a+RA — 88%

(FSC-H vs CD31 FITC flow cytometry plots)

C

CD31 — Fold Change (relative to BM)
CADH5 — Fold Change (relative to BM)
VEGFR2 — Fold Change (relative to BM)

- BM
- BM+VEGF
- BM+Wnt3a
- BM+RA
- BM+VEGF+Wnt3a
- BM+VEGF+Wnt3a+RA

D

- BM
- BM + VEGF
- BM + Wnt3a
- BM + RA
- BM + VEGF + Wnt3a
- BM + VEGF + Wnt3a + RA
- Coculture
- hCMEC/D3

Pe LY (10⁻³cm/min)

E

- BM
- BM + VEGF
- BM + Wnt3a
- BM + RA
- BM + VEGF + Wnt3a
- BM + VEGF + Wnt3a + RA
- Coculture
- hCMEC/D3

TEER (Ωxcm²) vs Time (days)

Figure 3

A Well plate (ca. 15-20 days) | Transwell (6 days)

P0   P1   P5

BM + VEGF_50 | BM
Fibronectin
Glial ECM
Brain endothelial cell ECM

BM + VEGF_50 | BM + Wnt3a_10 + VEGF_25 + RA_10 | BM + Wnt3a_10 + VEGF_25
Fibronectin
Glial ECM
Brain endothelial cell ECM

B

1= Fibronectin_BM+VEGF+Wnt+RA
2= Coculture
3= Fibronectin_BM
4= Glial ECM_BM+VEGF+Wnt+RA
5= Glial ECM_BM

Genes (heatmap rows):
LAMC1, LAMA4, LAMA5, LAMB1, COL4A1, COL4A2, HSPG2, FN1, ITGA1, ITGA3, ITGA4, ITGA5, ITGA6, ITGB3, ITGB4, SELE, ENOS, HO1, VWF, CD31, CD34, CADH5, VEGFR2, RARα, RARβ, RARγ, CCND3, CDK6, CDK4, P21, FZD6, FZD7, FZD4, DAMM1, WIF1, LEF1, APCDD1, NOTCH2, NOTCH4, NOTCH1, HES1, HEY1, TLE1, JAG1, CLDN1, CLDN3, CLDN5, OCLN, ZO1, PVLAP, SLC6A8, SLC3A2, SLC7A5, SLC7A1, SLC16A1, SLC44A5, SLC6A12, SLC2A1, ABCB1, ABCC1, ABCC2, ABCC4, ABCC5, ABCC8, ABCG2, TFRC, LRP1, STRA6, LDLR, INSR, LEPR

Scale: -0.5 (blue), +0.5 (red)

C Fibronectin | Glial ECM | bBCECs ECM

CLAUDIN-5
ZO-1
VE-CADHERIN

D

Fibronectin
bBCECs ECM
Glial ECM

Pe LY (10^-3 cm/min)

BM | BM+VEGF+Wnt3a+RA

** , **** significance markers

E

■ Fibronectin_BM
♦ Fibronectin_BM+VEGF+Wnt3a+RA
■ Glial ECM_BM
♦ Glial ECM_BM+VEGF+Wnt3a+RA
■ bBCECs ECM_BM
♦ bBCECs ECM_BM+VEGF+Wnt3a+RA

TEER ($\Omega \times cm^2$)

Time (days): 2, 4, 6

Figure 4

Table

GENE	Coculture			Fibronectin_BM	
	Replicate 1	Replicate 2	Replicate 3	Replicate 1	Replicate 2
LAMC1	0.01	0.36	0.31	0.2080754	0.1748912
LAMA4	0.43	0.27	0.43	0.0244888	0.0243505
LAMA5	8.60E-10	8.60E-10	8.60E-10	0.0177774	0.024476
LAMB1	0.52	0.29	0.36	0.2037681	0.1788163
COL4A1	0.57	0.53	0.35	0.120073	0.1005237
COL4A2	0.24	0.295	0.35	0.1984972	0.2147721
HSPG2	0.11	0.08	0.09	0.0520672	0.0342321
FN1	0.43	0.33	0.5	0.4110593	0.4357572
ITGA1	0.5	0.81	0.41	0.0315268	0.0323728
ITGA3	0.39	0.25	0.38	0.0416626	0.0428242
ITGA4	0.0037703	0.0048307	0.0041473	0.0036497	0.0037815
ITGA5	0.2474113	0.2406671	0.2346702	0.2007182	0.2059533
ITGA6	0.1234734	0.1212813	0.1384926	0.0568821	0.0637966
ITGB3	0.014971	0.0144476	0.0133762	0.001609	0.001512
ITGB4	0.006516	0.0066623	0.0066093	0.001192	0.001333
SELE	0.17	0.13	0.15	0.0004286	0.0004273
ENOS	0.12	0.13	0.11	0.0010967	0.0011863
HO1	0.33	0.32	0.3	0.0010452	0.0013145
VWF	0.51	0.59	0.66	0.0105478	0.0077146
CD31	1.29	1.66	1.45	0.1919129	0.147011
CD34	0.2	0.22	0.17	8.60E-10	8.60E-10
CADH5	1.98	1.87	1.5	0.170886	0.1067466
VEGFR2	0.4	0.36	0.51	0.1269032	0.1515768
RAR α	0.0017718	0.0022779	0.00202485	0.0001656	0.0001624
RAR β	0.0054485	0.0055757	0.0059613	0.0020095	0.0017925
RAR γ	0.0016008	0.0014768	0.0017386	0.0013452	0.0015327
CCND3	0.0190638	0.0230734	0.0211091	0.0134662	0.015738
CDK6	0.0016968	0.0017681	0.0018874	0.0026942	0.003201
CDK4	0.0224257	0.0265118	0.029957	0.0212923	0.0237725
P21	0.0343769	0.033075	0.0344278	0.0451669	0.0431464
FZD6	0.0283239	0.0300087	0.0351523	0.0319291	0.0274771
FZD7	0.0024924	0.0016078	0.0015166	0.0074708	0.0110909
FZD4	0.0262389	0.033078	0.0328472	0.0335578	0.0456592
DAAM1	0.0026953	0.0028115	0.0026515	0.0026161	0.0024734
WIF1	0.0022852	0.0025602	0.002774	0.0032219	0.0035341
LEF1	0.0023638	0.0023927	0.0026361	0.0035163	0.0041296
APCDD1	0.0032265	0.0031264	0.0028795	0.0042335	0.0061049
NOTCH2	0.0221597	0.0227585	0.0231667	0.0328768	0.0345658
NOTCH4	0.0056346	0.00603	0.0057102	0.0081565	0.0104707
NOTCH1	0.0221931	0.0239106	0.0221683	0.0055782	0.0060475
HES1	0.0070644	0.0067852	0.0067904	0.0058478	0.0053876
HEY1	0.0027559	0.0029579	0.0031825	0.0223736	0.0127722
TLE1	0.0072885	0.0082185	0.0077632	0.0060177	0.0058819
JAG1	0.0023624	0.0026437	0.002847	0.0091258	0.0082144

CLDN1	0.26	0.25	0.24	0.023775	0.0302541
CLDN3	0.21	0.195	0.18	0.010225	0.0120471
CLDN5	0.21	0.17	0.18	0.0337355	0.0449824
OCLN	0.19	0.2	0.18	0.0287055	0.0231153
ZO-1	0.52	0.46	0.5	0.0607216	0.079261
PVLAP	0.004741	0.005067	0.004717	0.0851592	0.0807441
SLC6A8	0.0085203	0.0088008	0.0085555	0.0061376	0.025782
SLC3A2	0.0209548	0.0235463	0.0240287	0.0506629	0.036713
SLC7A5	0.0076028	0.0087094	0.0094503	0.0539011	0.0678313
SLC7A1	0.0200733	0.019002	0.0218201	0.0355616	0.035123
SLC16A1	0.0820644	0.0832901	0.0895611	0.0566383	0.0484556
SLC44A5	0.0033085	0.0034407	0.0031059	0.0257598	0.0322203
SLC6A12	0.0013899	0.0011368	0.0012951	0.0294372	0.034052
SLC2A1	0.0052847	0.0060181	0.0080192	0.0204321	0.026559
ABCB1	0.02	0.01	0.01	0.0001505	0.0002508
ABCC1	0.72	0.78	0.52	0.063108	0.0762635
ABCC2	0.0009057	0.0010041	0.0011136	0.0002927	0.0003406
ABCC4	0.0073152	0.0086881	0.008488	0.0341069	0.0326823
ABCC5	0.0019961	0.0021611	0.002417	0.0167764	0.0171427
ABCC8	0.0015034	0.0017699	0.0014049	0.0027912	0.0023764
ABCG2	0.0044965	0.0051568	0.0056655	0.0271689	0.0173327
TFRC	0.02	0.01	0.02	0.0036778	0.0038024
LRP1	0.0011024	0.0014313	0.0013809	0.0248002	0.0250178
STRA6	0.0001115	0.0001411	0.0001439	0.0017875	0.0020454
LDLR	0.0113643	0.016622	0.0165687	0.0701862	0.066029
INSR	0.0008188	0.0007009	0.0006439	0.0083603	0.0058693
LEPR	0.0227315	0.0219813	0.0253756	0.0031889	0.0026983

Fibronectin_BM+VEGF+Wnt3a+RA				Glial ECM_BM		
Replicate 3	Replicate 1	Replicate 2	Replicate 3	Replicate 1	Replicate 2	Replicate 3
0.1758717	0.05	0.36	0.17	0.0968268	0.1130266	0.1236075
0.029361	0.38	0.44	0.41	0.0088751	0.0090241	0.010731
0.0253518	8.60E-10	8.60E-10	8.60E-10	0.0056022	0.0048074	0.0066031
0.2241798	0.41	0.46	0.39	0.0332444	0.0340268	0.0369525
0.1335473	0.4	0.42	0.43	0.0115579	0.0217275	0.0156625
0.2271317	0.66	0.34	0.98	0.0411367	0.0445679	0.0471857
0.0533889	0.07	0.06	0.06	0.0015381	0.0022256	0.0021897
0.3333553	0.12	0.12	0.14	0.2632743	0.3683409	0.3423858
0.0365294	0.44	0.33	0.37	0.0039319	0.0037659	0.0042168
0.0417447	0.21	0.35	0.28	0.0045362	0.004994	0.0051671
0.0037161	0.0024497	0.0024336	0.0024282	0.0016247	0.0018363	0.0017479
0.2053825	0.1228569	0.1028672	0.1052232	0.0141884	0.0153926	0.0145539
0.0607098	0.0750393	0.0847578	0.0786018	0.0560807	0.0566156	0.0602073
0.0016753	0.0274213	0.0221478	0.0199508	0.0003856	0.0004206	0.0003472
0.0014593	0.0004896	0.0007718	0.0008816	0.000231	0.0002031	0.0003134
0.0003075	0.0674114	0.0649862	0.0536557	0.0005513	0.0007231	0.0006501
0.0014973	0.13	0.07	0.06	0.0008572	0.0007932	0.0007191
0.0011894	0.11	0.15	0.13	0.0013921	0.0014127	0.0015985
0.0071885	0.1647178	0.0928456	0.1820099	0.0009837	0.0014695	0.0011464
0.2555988	1.76	1.53	1.49	0.0057547	0.0064423	0.0051443
8.60E-10	0.18	0.2	0.07	8.60E-10	8.60E-10	8.60E-10
0.1262563	1.34	1.44	1.5	0.0044425	0.0043458	0.0043099
0.1169202	1.053976	0.7283844	0.7834234	0.0555962	0.0532707	0.0559404
0.0001866	0.0021999	0.0006555	0.0007693	0.00002478	0.00003615	0.000065
0.0025639	0.0059319	0.0063018	0.0053511	0.0007975	0.0007629	0.0009827
0.0020463	0.01248685	0.0089872	0.0159865	0.0012355	0.0011451	0.0011125
0.014771	0.02424165	0.0279921	0.0204912	0.0042818	0.0026973	0.0029439
0.0040758	0.0046903	0.0031197	0.0040653	0.0008645	0.000962	0.0009692
0.0239655	0.0152918	0.0143581	0.0159243	0.0152128	0.0124446	0.0172394
0.0506757	0.0606946	0.0681741	0.0925418	0.0022103	0.0021732	0.0020548
0.0276445	0.0368141	0.045824	0.0463212	0.0030537	0.0028169	0.0027766
0.0095722	0.0014916	0.0017496	0.0016387	0.0146557	0.0161562	0.0161518
0.0394093	0.0259592	0.0232192	0.0281659	0.002104	0.0020711	0.0015084
0.0028424	0.0039126	0.0050475	0.0044607	0.0028199	0.0010985	0.0036741
0.0042447	0.0031601	0.0035422	0.0027059	0.0003097	0.0005218	0.0009666
0.0040149	0.0020054	0.0029905	0.0030747	0.0010255	0.0009117	0.0009989
0.0052124	0.0010778	0.0020014	0.0020171	0.0035067	0.0039816	0.0045071
0.0334527	0.0278437	0.0333912	0.0268838	0.0156534	0.018663	0.0165742
0.008513	0.0200836	0.0161307	0.0196678	0.0011871	0.0012465	0.0012801
0.0073756	0.0127162	0.0132742	0.0124084	0.0011263	0.0013271	0.0012745
0.0077955	0.0070679	0.0069374	0.0062895	0.0012441	0.0009693	0.001317
0.0175195	0.0351909	0.0344065	0.031882	0.001773	0.001794	0.0018873
0.0065315	0.0029905	0.0028049	0.0027534	0.0057411	0.0047768	0.0047842
0.0085979	0.0047364	0.0030631	0.0045967	0.001246	0.0014176	0.0015704

0.0262962	0.12	0.09	0.1	0.0003067	0.0003425	0.0003176
0.0140889	0.09	0.1	0.07	0.0001595	0.0001791	0.0002089
0.0365946	0.1080579	0.1001402	0.1102359	0.000314	0.0003937	0.000366
0.0302676	0.0911099	0.0755563	0.0862653	0.0099352	0.0101657	0.010261
0.0742482	0.21	0.19	0.24	0.0355571	0.0373763	0.0369489
0.0970963	0.0038113	0.0055318	0.0054614	0.0236118	0.009524	0.0193055
0.0078286	0.0044435	0.0056333	0.0062175	0.0026311	0.0034576	0.0026032
0.0520574	0.0160883	0.0158162	0.0177873	0.0100736	0.0144196	0.0135542
0.0640191	0.0105336	0.0098597	0.0107206	0.0211105	0.018684	0.0217666
0.0471843	0.0084513	0.0098186	0.0113584	0.0140093	0.0156265	0.0163101
0.0506017	0.0655201	0.0635155	0.0551728	0.0666161	0.0696286	0.0638416
0.0269905	0.0086525	0.0090108	0.0077535	0.001143	0.0011358	0.001336
0.0286745	0.0586075	0.0508928	0.05475015	0.0002222	0.0001511	0.0001721
0.0250216	0.0191442	0.0213381	0.2024115	0.0408631	0.0395774	0.0411413
0.0002007	0.01	0.01	0.01	0.0000297	0.00003508	0.00002939
0.0638266	0.35	0.38	0.41	0.0043161	0.0039759	0.0039537
0.0002661	0.002907	0.0036681	0.0027072	0.0001416	0.0001165	0.00005841
0.0335107	0.0105557	0.0115018	0.0098466	0.0016117	0.0019907	0.0020092
0.0169596	0.18	0.17	0.15	0.0022729	0.0025399	0.0025607
0.0025835	0.0020622	0.0028905	0.0025823	0.0007231	0.0007181	0.000383
0.0275722	0.0039792	0.0035112	0.004268	0.0014731	0.0014496	0.0018061
0.0037401	0.11	0.11	0.08	0.0234389	0.0213107	0.0241387
0.0266818	0.000715	0.000651	0.0005542	0.0277599	0.0212906	0.0261173
0.0018973	0.0027191	0.0039541	0.001564	0.0009266	0.0008134	0.0009013
0.0196271	0.25	0.35	0.28	0.0100698	0.011327	0.0134944
0.0071148	0.07	0.06	0.09	0.0005325	0.000582	0.000951
0.0028363	0.0037593	0.0042223	0.0031736	0.0009752	0.0009995	0.0013412

Glial ECM_BM+VEGF+Wnt3a+RA		
Replicate 1	Replicate 2	Replicate 3
0.1995329	0.2277803	0.2307142
0.0493733	0.059469	0.0622665
0.0327919	0.0323561	0.0337712
0.3592026	0.3881984	0.3974931
0.2498508	0.2594842	0.3131543
0.4572553	0.4684494	0.4166354
0.1730673	0.1765334	0.1902942
1.150149	1.023124	1.202861
0.0452503	0.0419131	0.0426019
0.0398084	0.0393911	0.0410996
0.0061288	0.006508	0.0064805
0.2971697	0.2897734	0.2888977
0.0550634	0.059148	0.0584081
0.0031983	0.0029544	0.0028395
0.001162	0.001329	0.001263
0.0022099	0.0017488	0.002583
0.0022094	0.0023386	0.0031933
0.0166296	0.0142603	0.0145762
0.0245484	0.0266072	0.0277683
0.5974333	0.7997014	0.6616338
0.0196962	0.0205508	0.0201235
0.300283	0.220707	0.288086
0.5142098	0.5920357	0.777026
0.0004729	0.0003363	0.0007788
0.0026502	0.0029503	0.0024606
0.0013394	0.0015926	0.0012683
0.0182693	0.0197517	0.0241993
0.0042364	0.0042109	0.0040364
0.0162506	0.0212218	0.021049
0.0599303	0.0808358	0.076125
0.0297678	0.0308955	0.0240106
0.0025516	0.0038123	0.0038317
0.1003626	1.385311	2.227694
0.0908648	0.0423314	0.0652568
0.0232291	0.0390589	0.0610004
0.0056068	0.0026273	0.0058862
0.0226712	0.0215741	0.021333
0.03819	0.0171094	0.0335314
0.0512629	0.0494537	0.0492248
0.0095193	0.0093626	0.0156759
0.0105937	0.0085457	0.0097412
0.0319573	0.0330839	0.0187827
0.0031139	0.0057068	0.0048008
0.0096321	0.008472	0.0090491

0.001205	0.0009652	0.0008942
0.0003431	0.000309	0.0003766
0.0328384	0.0325372	0.0355999
0.0080765	0.0082715	0.0085748
0.0535664	0.0518714	0.0540055
0.1207888	0.1292879	0.1529558
0.0067802	0.0087083	0.0082604
0.0591462	0.0464055	0.0656597
0.0315903	0.0297581	0.0277736
0.0447127	0.0552963	0.0556045
0.0539402	0.0577859	0.0599534
0.0089463	0.0141668	0.0136613
0.0007011	0.0008584	0.0006948
0.0234535	0.0224587	0.0234351
0.0001237	0.0003566	0.000183
0.0220073	0.0157826	0.0160004
0.0006604	0.000312	0.0011222
0.0092991	0.0079931	0.0097778
0.006021	0.0055441	0.0070497
0.0016065	0.001894	0.0042198
0.0073693	0.0125071	0.0090576
0.016102	0.0181434	0.0200326
0.0035028	0.0032136	0.0029565
0.0017559	0.0020245	0.0019064
0.0220165	0.0230645	0.0225405
0.0054632	0.0046946	0.0082447
0.00389	0.0050326	0.0038997

SUPPLEMENTAL INFORMATION

5 Supplemental data:
- S1, related to Figure 2.
- S2, related to Figure 3.
- S3 and S4, related to Figure 4.
- Table S1, related to Figure 3.

Supplemental Experimental Procedures

Supplemental References, related to Supplemental Experimental Procedures

2 Supplemental Tables
- Table S2, sequence of primers used in this study.
- Table S3, primary and secondary antibodies used in this study.
- Table S4, main products used in this study.
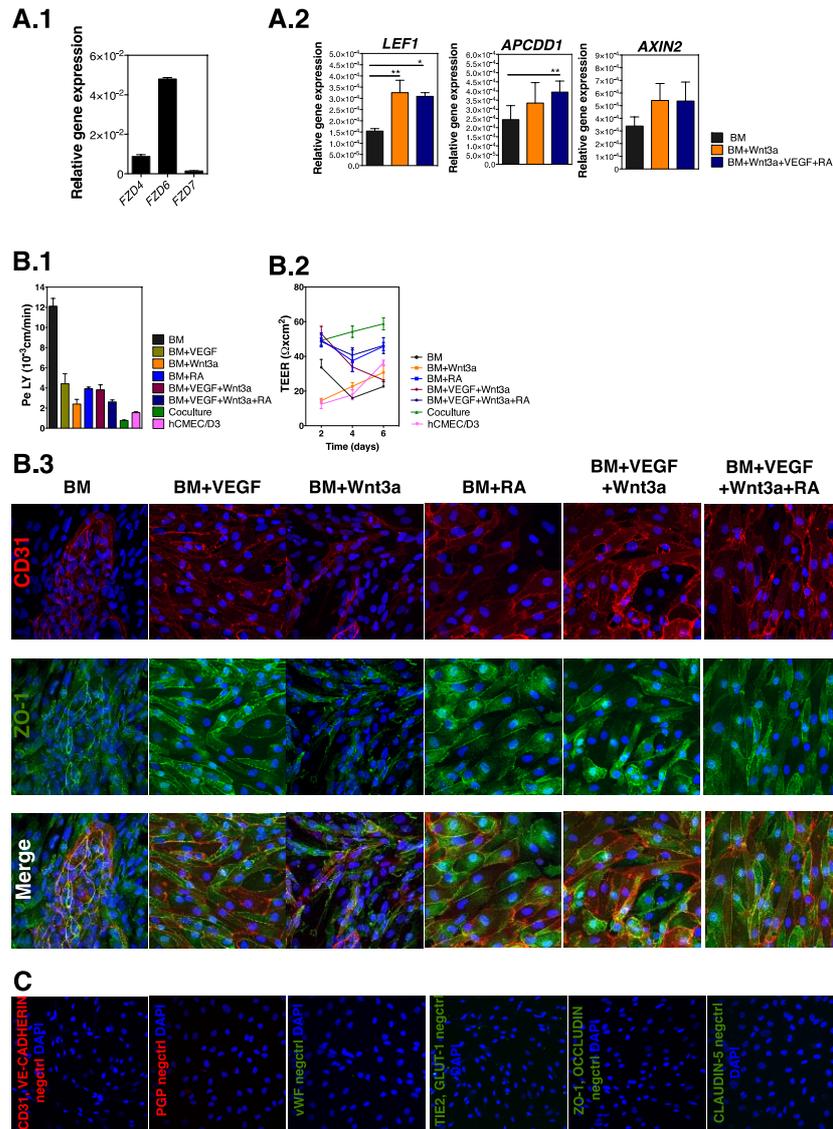
Supplemental data items

Figure S1 – Gene expression of WNT pathway genes and functional characterization of non-purified endothelial cells after 6 days of culture in a transwell insert (related to Figure 2).

(A.1). Relative gene expression of frizzled receptors (*FZD4*, *FZD6* and *FZD7*) in CD31-ECs at passage 1. Mean ± SEM (n=1 independent experiment, 3 technical replicates per experimental condition).

(A.2) Relative expression of *LEF1*, *AXIN2* and *APCDD1* genes in CD31+ cells at passage 1 exposed to basal medium (BM) or to Wnt3a (BM+Wnt3a or BM+VEGF+Wnt3a+RA; 10 ng/mL of Wnt3a) for 24 h. Mean ± SEM (n=3 independent experiments, 3 technical replicates per experimental condition). *$P<0.05$ and **$P<0.01$ using one-way ANOVA followed by Dunnett's multiple comparison test.

(B.1) Paracellular permeability of cells to LY after 6 days of culture on Matrigel-coated filters. As controls we have used the hCMEC/D3 cell line and human hematopoietic progenitor cells derived ECs cocultured with pericytes (Coculture condition). Values are Mean ± SEM (n=2 independent experiments, at least 3 transwell inserts per independent experiment and experimental condition).

(B.2) TEER at different time points for all the conditions tested on Matrigel-coated filters. As controls we have used the hCMEC/D3 cell line and human hematopoietic progenitor cells derived ECs cocultured with pericytes (Coculture condition). Values are Mean ± SEM (n=2 independent experiments, at least 3 transwell inserts per independent experiment and experimental condition).

(B.3) Co-localization of CD31 and ZO-1 markers in the cells after 6 days of culture on Matrigel-coated filters. Scale bar is 50 μm.

(C) Controls (without primary antibodies) for immunostaining analyses. Scale bar is 50 μm.
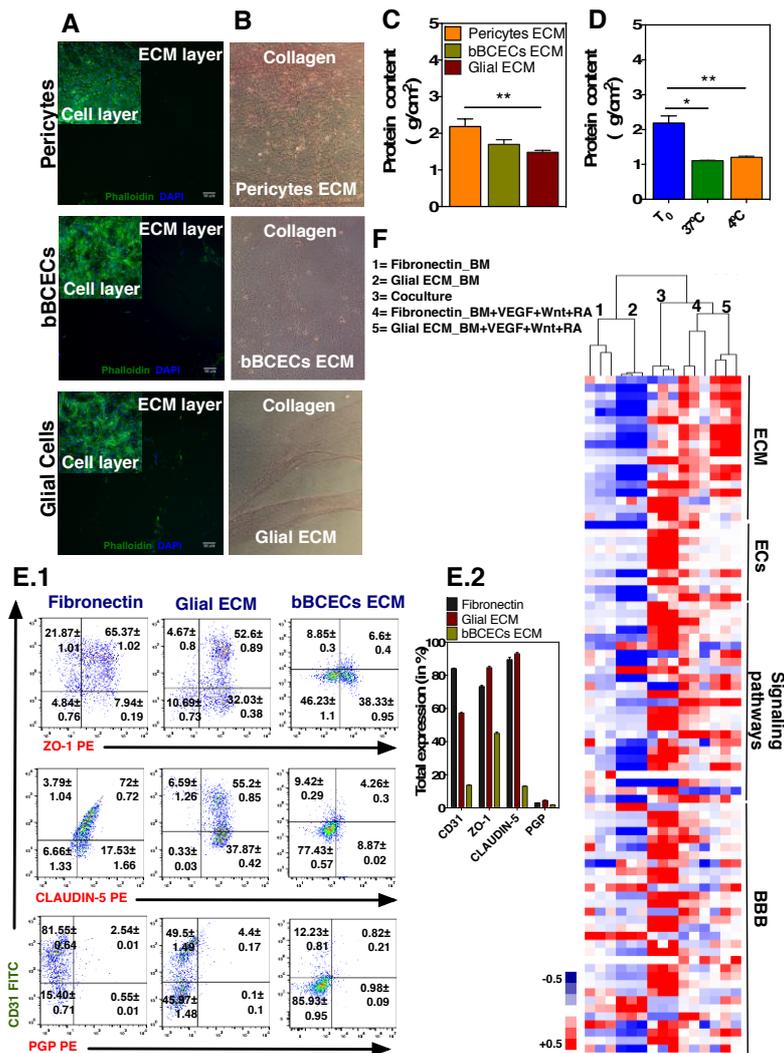
Figure S2 – Isolation and characterization of decellularized ECM from cells of the neurovascular unit and characterization of BCLECs matured in these matrices in the presence of soluble factors (related to Figure 3).

(A) Evaluation of the decellularization protocol efficacy by staining with DAPI and phalloidin. Scale bar is 50 μm.

(B) Evaluation of collagen by Sirius red assay.

(C) Comparison of ECM production from bovine pericytes, bovine brain capillary endothelial cells (bBCECs) and rat glial cells at day 8. Values are Mean ± SEM (n= 3 independent experiment, 3 individual wells per experimental condition). **P<0.01* using one-way ANOVA followed by Tukey's multiple comparison test.

(D) Stability of the native pericytes ECM at 37°C and 4°C in terms of maintenance of the collagen content. Values are Mean ± SEM (n= 3 independent experiment, 3 individual wells per experimental condition). *P<0.05* and **P<0.01* using One-way Anova followed by Tukey's multiple comparison test.

(E.1) Expression by flow cytometry of BBB markers (ZO-1, CLAUDIN-5 and PGP) co-localized with CD31 marker in cells matured on fibronectin or decellularized matrices at passage 4. Percentages of positive cells were calculated based in the isotype controls (1%).

(E.2) Total expression of each cell marker in the different assessed conditions. Values are Mean ± SEM (n=1 independent experiment, 3 individual wells per experimental condition).

(F) Heatmap and hierarchical clustering dendogram in gene expression results obtained by Fluidigm**.** Relative gene expression levels on cells cultured on BM or BM+VEGF+Wnt3a+RA either on fibronectin or glial ECM (positive control was "coculture" condition, i.e., human hematopoietic stem/progenitor-derived ECs cocultured with pericytes, please see ref (Cecchelli et al., 2014) followed by their plating on Matrigel-coated transwell inserts for 6 days. Genes were normalized against the control gene *β-ACTIN* (n=1 independent experiment, 3 technical replicates per experimental condition). For each gene, the normalized values were between +0.5 and -0.5 (please see Supplementary Information for further information). Gene expression that was above the gene expression median for all the experimental groups was shown in red, the expression below the median in blue and the expression similar to the median in white.
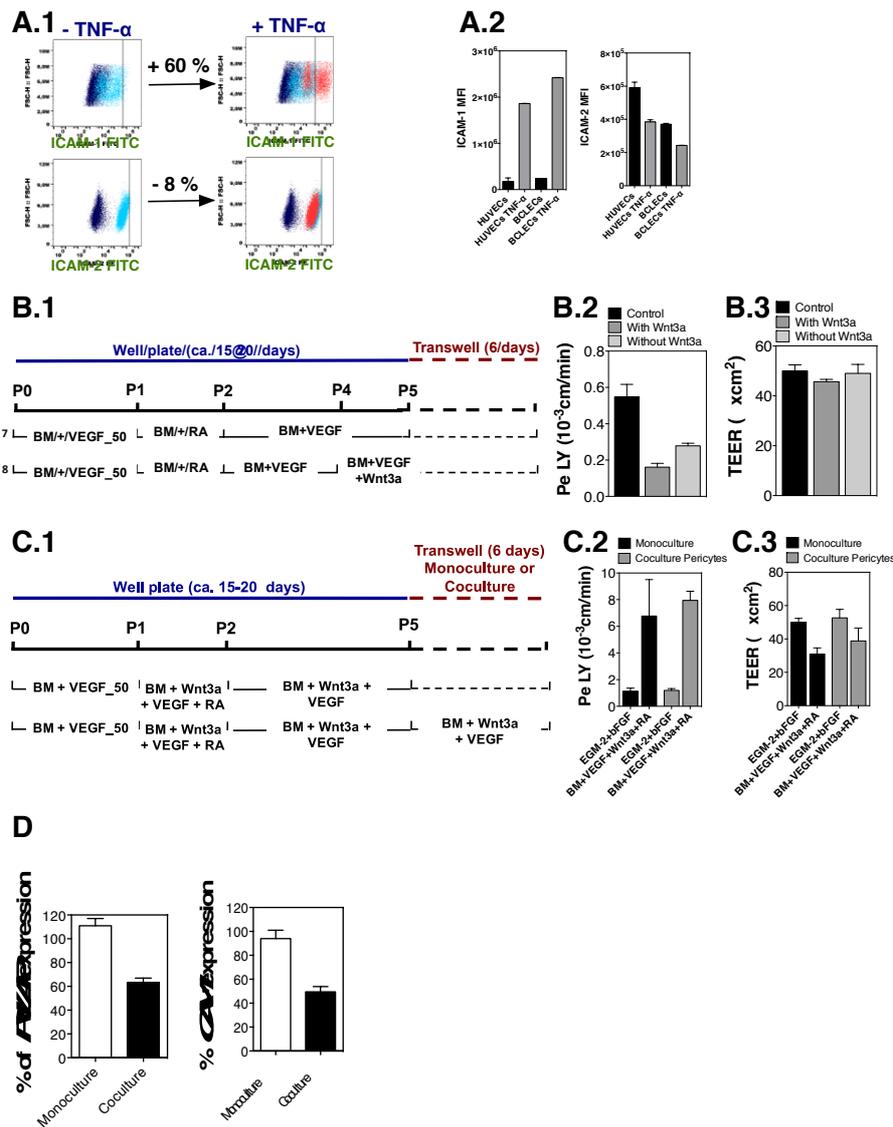
Figure S3 – Characterization of BCLECs and control cells (related to Figure 4).

(A) Immunofluorescence analyses for the co-localization of CD31 with ZO-1 proteins in BCLECs at passage 2 and 4 on fibronectin-coated plates. Scale bar is 50 μm.

(B.1) Expression of BCEC markers in HUVECs by flow cytometry. Percentage of positive cells were calculated based in the isotype controls (1%; dark blue scatter plot).

(B.2) Immunofluorescence analyses of BCEC markers in HUVECs. Scale bar is 50 μm.

(C) Expression of BCEC markers in hCMEC/D3 by flow cytometry. Percentage of positive cells were calculated based in the isotype controls (1%; light blue scatter plot).

(D.1) Characterization of BCLECs derived from a human embryonic stem cell line (hESCs-NKX2-5eGFP/W) by flow cytometry. Cells were cultured in BM+VEGF+Wnt3a+RA media for 4 passages. Percentages of positive cells were calculated based in the gates defined by the isotype control (1%).

(D.2) Characterization of BCLECs derived from a human embryonic stem cell line (hESCs-NKX2-5eGFP/W) by immunofluorescence. Immunofluorescence analyses for CD31, ZO-1 and CLAUDIN-5 on cells platted on Matrigel-coated filters. Scale bar is 50 μm.

(E.1) Characterization of BCLECs derived from iPSCs cell line (HGPS-iPSCs) by flow cytometry. Cells were cultured in BM+VEGF+Wnt3a+RA media for 4 passages. Percentages of positive cells were calculated based in the gates defined by the isotype control (1%).

 (E.2) Characterization of BCLECs derived from a iPSCs cell line (HGPS-iPSCs) by immunofluorescence. Immunofluorescence analyses for CD31, ZO-1 and CLAUDIN-5 on cells platted on Matrigel-coated filters. Scale bar is 50 μm.

Figure S4 – Functional Characterization of BCLEC (related to Figure 4).

(**A.1**) Expression of adhesion molecules (ICAM-1 and ICAM-2) in HUVECs at basal level and after exposure to TNF-α (10 ng/mL) for 24 h, by flow cytometry. Percentage of positive cells were calculated based in the shift of the basal expression for each marker (1%; light blue scatter plot).

(**A.2**) Expression of ICAM-1 and ICAM-2 by mean intensity fluorescence (MFI; flow cytometry) in HUVECs and BCLECs at basal level and after exposure to TNF-α (10 ng/mL) for 24 h. Results are Mean ± SEM (n=1 independent experiment, 3 technical replicates per experimental condition).

(**B.1**) Protocol used to assess the impact of Wnt3a at later stages of the specification.

(**B.2**) Paracellular permeability to LY at day 6 in the transwell system. Results are Mean ± SEM (n=1 independent experiment, with 3 transwell inserts per experimental condition). Control are BCLECs derived with protocol 6.

(**B.3**) TEER at day 6 in the transwell system. Results are Mean ± SEM (n=1 independent experiment, with 3 transwell inserts per experimental condition). Control are BCLECs derived with protocol 6.

(**C.1**) Protocol used to assess the impact of pericytes coculture.

(**C.2**) Paracellular permeability to LY at day 6 in the transwell system. Results are Mean ± SEM (n=1 independent experiment, with 3 transwell inserts per experimental condition).

(**C.3**) TEER at day 6 in the transwell system. Results are Mean ± SEM (n=1 independent experiment, 3 filters per condition).

(**D**) Relative gene expression of *PVLAP* and *CAV-1* in BCLECs (cells differentiated with BM+VEGF+Wnt3a+RA) in filters in monoculture or coculture with pericytes at day 6. Data was normalized by day 3 in filters for each condition. Genes were normalized against the control gene *β-ACTIN*. Results are Mean ± SEM (n=1 independent experiment, 3 technical replicates per experimental condition).

Table S1 – Relative gene expression data for heatmap (in Excel format). The gene expression was normalized against the endogenous control *(β-ACTIN)* and presented as relative gene expression**.** Related with Figure 3.

SUPPLEMENTAL EXPERIMENTAL PROCEDURES

Cultivation of pluripotent stem cells and differentiation into EPCs.
Pluripotent stem cells were kindly donated from several collaborators. K2-iPSC cell line generated from human cord blood (passages: 30-40) (Haase et al., 2009) and Hutchinson-Gilford Progeria Syndrome (HGPS) cell line generated from fibroblasts (passages: 43-51) (Nissan et al., 2012). For certain experiments the human embryonic stem cell line hESCs-NKX2-5$^{eGFP/W}$ (passages: 40-45) (Elliott et al., 2011) was used. Pluripotent stem cells were grown on mitomycin C-inactivated mouse embryonic fibroblast feeder layer in undifferentiating culture medium [(knockout Dulbecco's Modified Eagle Medium; DMEM (GIBCO)], 20% knockout serum replacer (Gibco), non-essential amino acids (1%, GIBCO), β–mercaptoethanol (0.1 mM, Sigma), L-glutamine (1 mM, Sigma), Pen/Strep (50 U/mL:50 μg/mL, Lonza) and fibroblast growth factor-basic (bFGF; 5 ng/mL, Preprotech). iPSCs (at passages 27-35) were passaged every 3-4 days with collagenase IV (1mg/mL, Gibco) at a typical split ratio of 1:4 or 1:6. To initiate the differentiation, iPSCs ($27{\times}10^3$ – $45{\times}10^3$ cells per cm^2) were treated for 45-60 min with collagenase IV and plated on fibronectin-coated dishes (1 μg/cm^2; Calbiochem) in a chemically defined medium (CDM) (Vallier et al., 2009) containing Iscove's Modified Dulbecco's Medium (IMDM; 50% (v/v), Gibco), F12 (50%, Gibco), BSA (5 mg/mL, Sigma), β-mercaptoethanol (0.1 mM, Sigma), Pen/Strep (50 U/mL:50 μg/mL, Lonza), transferrin (15 mg/mL, Sigma) and insulin (7 mg/mL, Sigma). Immediately after cell seeding, to induce mesoderm differentiation, cells were exposed to bone morphogenetic protein 4 (BMP4, 10 ng/mL, Peprotech) for 1.5 days and then BMP4 (50 ng/mL, Peprotech) with bFGF (20 ng/mL, Peprotech) for 3.5 days. To differentiate mesoderm progenitor cells into endothelial cells, cells were cultured with vascular endothelial growth factor (VEGF$_{165}$;50 ng/mL, Peprotech) and thymosin β4 (Tβ 4; 100 ng/mL, Caslo peptide synthesis). CD31$^+$ cells were isolated by Magnetic-Activated Cell Sorting (MACS; Miltenyi Biotec) (Rosa et al., 2019). CD31$^+$ enrichment was confirmed by flow cytometry analyses using a different anti-CD31 antibody (eBiosciences), with a positivity superior to 90%.

Preparation of decellularized ECM.
We have prepared decellularized ECM from three different primary cells types: bovine pericytes, bovine brain capillary endothelial cells (bBCECs) and rat glial cells. Cells were platted on fibronectin-coated dishes (25 μg/mL; 1.7 μg/cm^2 of fibronectin adsorbed to the culture dish as quantified by immunocytochemistry) at a cell density of $3{\times}10^4$ cells per cm^2 during 8-12 days to allow extracellular matrix deposition. Cell layers were then decellularized using a solution of 20 mM ammonium hydroxide (Sigma) in PBS supplemented with 0.5% Triton X-100 (Fluka). After 1 min with agitation in contact with the solution, the resulting ECM layers were washed 2x with PBS and 1x with EGM-2. ECM layers were either used immediately or stored at 4°C. Approximately 10% (i.e. 0.17 μg/cm^2 of fibronectin) of the initial bovine fibronectin was still adsorbed to the cell culture dish after the decellularization (data not shown).

Endothelial permeability measurements.
To perform the assay, 10 $x10^4$ cells were seeded on a 12-well 0.4 μm filters (Costar) coated with Matrigel and kept in culture with EGM-2 supplemented with bFGF (1 ng/mL) for 6 days. Before initiating the permeability experiment, EBM-2 was added to empty wells of a 12-well plate. Filter inserts containing the BCLECs were placed in the multi-well and filled with EBM-2 containing the fluorescent integrity marker Lucifer yellow (LY; 20 μM, Sigma). The plates were placed on an orbital shaker for 1 h and then withdraw from the receiver compartment. The fluorescence of the samples (inserts with cells and without cells) was quantified using the wavelengths 430/530 (excitation/emission). The permeability values were generated through the blue-norna brain exposure simulator (http://www.blue-norna.com).

TEER analyses.
BCLECs TEER (Ohmxcm²) on Transwell filters was measured using the Millicell-ERS 2 (Electrical Resistance System, Millipore). The resistance of Matrigel-coated inserts was subtracted from the resistance obtained in the presence of the endothelial cultures according to the followed equation: TEER = [(TEER, cells)-(TEER, insert)×A], where A is the area of the filter (cm^2).

Dil-acLDL uptake
Cells were platted at a density of 10 $x10^4$ cells and 24 h later Dil-acLDL (Harbor Bio-Products, 20 μg/mL) was added to the cells for 4 h at 37ºC. At the end, Hoechst dye (0.25μg/ml) was added to stain cell nuclei. Cells were washed and kept in EGM-2. Images of the cells were acquired by a InCell Analyser HCA System.

Immunocytochemistry analyses.
Cells were fixed in cold methanol/acetone (50%/50%, v/v) for 5 min or with 4% (v/v) paraformaldehyde (PFA; electron Microscopy Science) for 10 min at room temperature and permeabilized with Triton X-100 (0.1%, v/v, Fluka) for 10 min, whenever required. The cells were then blocked with BSA (1%, w/v, Sigma) solution for at least 30 min followed by incubation with primary antibody (Table S3) during 1 h at RT. After washing, the cells were stained with secondary antibody (Table S3) for 30 min in dark at room temperature. The nuclei of the cells were counterstained with DAPI

(Sigma) and cells mounted with cell-mounting medium (DAKO). All the photos were taken using confocal microscopy (Zeiss) with an 40x oil objective.

Flow cytometry analyses.
Cells were dissociated from the culture plate by exposure to Cell Dissociation Buffer (Life Technologies) for 10 min and gentle pipetting, centrifuged and ressuspended in PBS supplemented with 5% (v/v) FBS (GIBCO). The single cell suspensions were aliquoted, fixed with ice-cold methanol/acetone (50%/50% v/v) or 1% (v/v) PFA and permeabilized with 0.5% (v/v) Tween, whenever necessary. The cells were stained with specific primary antibodies (Table S3). Cells were further incubated with the secondary antibody when necessary. For the co-localization experiments, ZO-1 and claudin-5 primary antibodies were conjugated with a R-Phycoerythrin (Abcam) dye to facilitate the setup of the experiment. Percentages of positive cells were calculated based in the isotype controls (1% of overlap with the isotype scatter plot). FACS Calibur and Accuri C6 were used for the acquisition and FlowJo was used for data analysis.

Expression of adhesion molecules in the BCLECs.
The expression of the adhesion proteins was assessed by flow cytometry. After the maturation of the cells for 4 passages in the presence of all soluble factors, the cells were purified for CD31 marker and plated on Matrigel-coated filters. After 5 days in the filters, the cells were exposed to Tumor Necrosis Factor-α (TNF-α) (10 ng/mL) for 24 h. The subsequent protocol was performed as previously described for flow cytometry experiments. The single cell suspensions were aliquoted and cells were stained with specific primary antibodies (Table S3). Cells were further incubated with the secondary antibody when necessary (Table S3). Non-treated cells were used to determine the basal expression of adhesion proteins. HUVECs were used as a control.

Total RNA extraction and quantitative real-time polymerase chain reaction (qRT-PCR) analyses.
Total RNA was isolated with a RNeasy Micro Kit (Quiagen) and quantified by a NanoDrop ND-1000 spectrophotometer (NanoDrop Technologies, Inc., USA) at 260 nm. The cDNA was reverse transcribed from total RNA using TaqMan reverse transcription reagents kit (Invitrogen) according to manufacturer instructions. qPCR reactions (10 μL) were prepared using NZY Speedy qPCR Green Master Mix (2x, 5 μL) (Nzytech), primers at a final concentration of 400 nM (1 μL each sequence), water (2 μL) and cDNA (1 μL). The qPCR was run in CFX Connect Real-Time System (BioRad). qPCR reactions in triplicate were performed for each qPCR experiment. Ct data were obtained using Bio-Rad CFX Manager Software. Relative quantification of the target was calculated relative to the housekeeping gene β-ACTIN. The $2^{--\Delta Ct}$ values (relative to the housekeeping gene) were used for the heatmap and hierarchical clustering analyses. The genes and primers sequences are given in Table S2.

qPCR using the high-throughput platform BioMarkTM HD System –Fluidigm
The oligos were designed for human transcripts and were synthesized by Sigma. Each RNA sample was diluted to the same concentration (15 ng/μL) and 1 μL was used to perform Retro transcription reactions. Fluidigm Reverse Transcription Master Mix (1 μL) was added to diluted RNA sample (1 μL) and water (3 μL) to a final volume of 5 μL. To perform the Pre-amplification (PA) of the cDNA samples a pool of primers was prepared. The primers were dissolved at a concentration of 100 μM in water. For each assay, a Primer Pair Mix was prepared containing 50 μM Forward Primer and 50 μM Reverse Primer. In order to prepare 10 × Pre-amplification Primer Mix (500 nM each primer), 10 μL of each of the 96 Primer Pair Mixes (50 μM each primer) was mixed with 40 μL buffer consisting of 10 mM Tris–HCl, pH 8.0; 0.1 mM EDTA; 0.25% Tween-20. In order to prepare 10× Assay (5 μM each primer) each Primer Pair Mix was diluted by mixing 10 μL Primer Pair Mix (50 μM each primer) with 90 μL buffer consisting of 10 mM Tris–HCl, pH 8.0; 0.1 mM EDTA; 0.25% Tween-20. PA reaction for each cDNA sample was prepared by mixing PreAmp Master Mix (1 μL, Fluidigm), pooled primers (500 nM, 0.5 μL), H$_2$0 (2.25 μL) and cDNA (1.25 μL). Thermal cycling was performed according to the manufacturer for 18 PA cycles. The samples were then treated with Exonuclease (New England Biolabs) to remove non-hybridized primers. The Fluidigm® 96.96 Gene expression IFC was used with EvaGreen chemistry. After a prime of the chip, a 10× assay mix and sample mix were prepared and pipetted into the inlets. The qRT-PCR on the preamplified samples was then carried out with a single pair of primers specific for the target, so non-specific interactions were likely negligible. The chip was loaded and data was collected using the BioMark HD^{TM}. Data were analyzed using Fluidigm® Real Time PCR Analysis v2.1 software and genes were normalized against β-ACTIN. Genes with melting curves displaying more of one peak (amplification of non-specific products) were not included in the analysis. The genes and primers sequences are given in Table S2.

Heatmap and hierarchical clustering analyses
The data processed by the Cluster 3.0 program was initially centered and then normalized. First, each individual gene expression ($2^{-\Delta Ct}$) (e.g. gene A) was subtracted to the gene expression median (e.g. gene A) for all experimental conditions. At the end, this creates a range of values for each gene so that the median value for all the experimental conditions is 0. Second, the centered values of each gene were normalized, by multiplying each centered value by a scale factor

(calculated by the program; a separate scale factor is computed for each gene) so that the sum of the squares of each value, for all experimental conditions, is 1.0. Therefore, for each gene the normalized values were between +1 to -1. The expression that is above the median is shown in red, the expression below the median in blue, and the expression similar to the median in white. The assembling of the data in terms of heatmap was performed in Java TreeView v1.1 software. The relative gene expression per condition for Figure 3B is given in Table S1.

Stain for actin cytoskeleton and nuclear DAPI.
To visualize the actin cytoskeleton and nuclear DAPI in a confluent cell layer and in ECM layer post decellularization, we fixed the plates with 4% PFA and permeabilize with 0.1% Triton X-100. Samples were then incubated with phalloidin-fluorescein (50 µg/mL, Sigma) for 40 min and washed twice. The nuclei were counterstained with DAPI and kept in mounting medium. All the photos were taken with the objective of 20x in the In Cell Analyzer 2200.

Stain for collagen and non-collagenous proteins.
Total amount of collagen in the decellularized ECM was quantified using Sirius Red/Fast Green Collagen staining kit (Chondrex) according to the manufacturer's instructions. The amount of sulfated glycosaminoglycans (sGAG) was quantified by staining with 1,9-dimethylmethylene blue dye (Blyscan Glycosaminoglycan Kit, Biocolor).

Coculture experiments.
Bovine pericytes, characterized elsewhere (Cecchelli et al., 2014), were immortalized using a SV40 large T antigen strategy (P7-P10). Immortalized cells were defrosted into a 100-mm gelatin-coated petri dish and cultured in Dulbecco's Modified Eagle's Medium (DMEM; Sigma) supplemented with FBS (20%, v/v), L-glutamine (2 mM), geneticin (200 µg/mL, G418, Sigma) and bFGF (1 ng/mL). Pericyte culture was confluent within 2-3 days. Once cells reached confluency, 45×10^3 were seeded into each well of 12-well plates (Costar). Endothelial cells cultured in 100-mm fibronectin-coated dishes for 4 passages with protocol 6 were trypsinized and purified using CD31 MACS beads. Cells were seeded at a cell density of 10×10^4 in 0.4 µm filters (Costar) coated with Matrigel and kept in culture with EGM-2 supplemented with bFGF (1 ng/mL) for 6 days.

Multidrug resistance accumulation assay.
Six days after being plated on polycarbonate filters, endothelial cell monolayers were washed with pre-warmed HEPES-buffered Ringer's (RH) solution (NaCl 150 mM, KCl 5.2 mM, CaCl$_2$ 2.2 mM, MgCl$_2$ 0.2 mM, NaHCO$_3$ 6 mM, Glucose 2.8 mM, HEPES 5 mM) with 0.1 % human serum albumin (Sigma). Cells were incubated with RH solution containing Rhodamine123 at a final concentration of 5 µM with or without Pgp inhibitor (0.5 µM elacridar). After 2 h in shaking conditions, Transwell filter with monolayer cells were placed on ice and the cells were washed five times with ice-cold RH solution. Cells were then lysed with RIPA lysis buffer (Millipore) for 3 min at 37°C and 200 µL were transferred to a 96 well-plate for measurements. The fluorescence of the samples was quantified using the wavelengths 501/538 (excitation/emission). Data were normalized against the control (cells without elacridar).

SUPPLEMENTAL REFERENCES
Haase, A., Olmer, R., Schwanke, K., Wunderlich, S., Merkert, S., Hess, C., Zweigerdt, R., Gruh, I., Meyer, J., Wagner, S., Maier, L. S., Han, D. W., Glage, S., Miller, K., Fischer, P., Schöler, H. R. and Martin, U. (2009). Generation of Induced Pluripotent Stem Cells from Human Cord Blood. Cell Stem Cell *4*, 434-441.
Nissan, X., Blondel, S., Navarro, C., Maury, Y., Denis, C., Girard, M., Martinat, C., De Sandre-Giovannoli, A., Levy, N. and Peschanski, M. (2012). Unique preservation of neural cells in Hutchinson- Gilford progeria syndrome is due to the expression of the neural-specific miR-9 microRNA. Cell reports *1*, 1-9.
Elliott, D. A., Braam, S. R., Koutsis, K., Ng, E. S., Jenny, R., Lagerqvist, E. L., Biben, C., Hatzistavrou, T., Hirst, C. E., Yu, Q. C., Skelton, R. J., Ward-van Oostwaard, D., Lim, S. M., Khammy, O., Li, X., Hawes, S. M., Davis, R. P., Goulburn, A. L., Passier, R., Prall, O. W., Haynes, J. M., Pouton, C. W., Kaye, D. M., Mummery, C. L., Elefanty, A. G. and Stanley, E. G. (2011). NKX2-5(eGFP/w) hESCs for isolation of human cardiac progenitors and cardiomyocytes. Nat Methods *12*, 1037-40.
Vallier, L., Touboul, T., Brown, S., Cho, C., Bilican, B., Alexander, M., Cedervall, J., Chandran, S., Ahrlund-Richter, L., Weber, A. and Pedersen, R. A. (2009). Signaling pathways controlling pluripotency and early cell fate decisions of human induced pluripotent stem cells. Stem cells (Dayton, Ohio) *11*, 2655-66.
Cecchelli, R., Aday, S., Sevin, E., Almeida, C., Culot, M., Dehouck, L., Coisne, C., Engelhardt, B., Dehouck, M. P. and Ferreira, L. (2014). A stable and reproducible human blood-brain barrier model derived from hematopoietic stem cells. PLoS One *6*, e99733.
Rosa, S., Praca, C., Pitrez, P. R., Gouveia, P. J., Aranguren, X. L., Ricotti, L. and Ferreira, L. S. (2019). Functional characterization of iPSC-derived arterial- and venous-like endothelial cells. Sci Rep *1*, 3826.

SUPPLEMENTAL TABLES

Table S2 - Details of primers for qRT-PCR and Fluidigm. Related to Figure 2, Figure 3, Figure 4, Figure S1 and Figure S4.

GENE	SENSE	ANTISENSE
ABCB1	TGAATCTGGAGGAAGACATGAC	CCAGGCACCAAAATGAAACC
ABCC1	AATAGAAGTGTTGGGCTGAG	CGAGACACCTTAAAGAACAG
ABCC2	ATATAAGAAGGCATTGACCC	ATCTGTAGAACACTTGACCA
ABCC4	AATCTACAACTCGGAGTCCA	CAAGCCTCTGAATGTAAATCC
ABCC5	ATTCTGATGTGAAACTAACAG	TTCCTATGTCGATATCCTTC
ABCC8	GATCATTGTGGGTGTGATTC	AGCCAGTAGAATGATGACAG
ABCG2	CAAGATGATGTTGTGATG	GATTCGTCATAGTTGTTG
APCDD1	GGAGTCACAGTGCCATCACAT	CCTGACCTTACTTCACAGCCT
AXIN2	AAAGAGAGGAGGTTCAGATG	CTGAGTCTGGGAATTTTTCTTC
CADH5	CGCAATAGACAAGGACATAAC	TATCGTGATTATCCGTGAGG
CAV1	GATTGACTTTGAAGATGTGATTG	AGAGAATGGCGAAGTAAATG
CCND3	AGACCAGCACTCCTACAG	GGCTTAGATGTGGTGTGG
CD31	AGATACTCTAGAACGGAAGG	CAGAGGTCTTGAAATACAGG
CD34	TGAAGCCTAGCCTGTCACCT	CGCACAGCTGGAGGTCTTAT
CDK4	TACCTGAGATGGAGGAGTC	GCAGAGATTCGCTTGTGT
CDK6	GAAAAGTGCAATGATTCTGGA	GAAGCGAAGTCCTCAACA
CLDN1	GAAAGACTACGTGTGACA	GGTCCTAATGTTAATGATAGTATC
CLDN3	ATCACGTCGCAGAACATC	TACACCTTGCACTGCATCTG
CLDN5	TTAACAGACGGAATGAAGTT	AAGCGAAATCCTCAGTCT
COL4A1	AAAGGGAGATCAAGGGATAG	TCACCTTTTTCTCCAGGTAG
COL4A2	AAAAGGAGATAGAGGCTCAC	GTATTCCGAAAAATCCAGCC
DAAM1	GAAGAAGAAAGCATTCCTCAG	CAGTTTGTTCTCGGGCAG
ENOS	AACGTGGAGATCACCGAG	GGGCAGAAGGAAGAGTTC
SELE	AGCTTCCCATGGAACACAAC	CTGGGCTCCCATTAGTTCAA
FN1	CCATAGCTGAGAAGTGTTTTG	CAAGTACAATCTACCATCATCC
FZD4	TACCTCACAAAACCCCCATCC	GGCTGTATAAGCCAGCATCAT
FZD6	TCGTCAGTACCATATCCCATG	CCCATTCTGTGCATGTCTTTT
FZD7	GATGATAACGGCGATGTGA	AACAAAGCAGCCACCGCAGAC
HES1	GCCTATTATGGAGAAAAGACG	CTATCTTTCTTCAGAGCATC
HEY1	CCGGATCAATAACAGTTTGTC	CTTTTTCTAGCTTAGCAGATCC
INSR	TGTTCATCCTCTGATTCTCTG	GCTTAGATGTTCCCAAAGTC
HO1	GAAAAGCACATCCAGGCAAT	GCTGCCACATTAGGGTGTCT
HSPG2	CCACTACTTCTATTGGTCCC	GTATTGGATTGGTGGAGATTAC
ITGA1	CAGGTTGGAATTGTACAGTATG	TGTCTATTCCAAGAGCTGTC
ITGA3	AGGTAATCCATGGAGAGAAG	GTAGAAGTTCTCATCCACATC
ITGA4	AAAGCTTGGATCGTACTTTG	CTCTTCCTTCCTCTCTGATG

Gene	Forward primer	Reverse primer
ITGA5	AAGCTTGGATTCTTCAAACG	TCCTTTTCAGTAGAATGAGGG
ITGA6	AAATACCAAACCAACACAGG	TACTGAATCTGAGAGGGAAC
ITGB3	AATCTGCTGAAGGATAACTGT	CTCTGGGGACTGACTTGA
ITGB4	ATCTGGACAACCTCAAGAAG	GCCAAATCCAATAGTGTAGTC
JAG1	GTCTCAAAGAAGCGATCAG	ATATACTCCGCCGATTGG
LAMA4	GAAATTGCATTTGAAGTCCG	ACCTGTCCATTTTTCATGTG
LAMA5	ATCCTATGACTTCATCAGCC	TTGTTATAGAAGAGGGAGAGG
LAMB1	GTGTGTATAGATACTTCGCC	AAAGCACGAAATATCACCTC
LAMC1	TCTCCTCTACCTTTCAGATTG	GGTTCTGACCATAACTCAAC
LDLR	GCCATTGTCGTCTTTATGTC	AAACACATACCCATCAACGA
LEF1	AAGGAACACTGACATCAATT	TTTGGAACTTGGCTCTTG
LEPR	GGAAATCACACGAAATTCAC	GCACGATATTTACTTTGCTC
LRP1	GACTACATTGAATTTGCCAGCC	TCTTGTGGGCTCGGTTAATG
MFSD2A	CAAACTTATTACTGGCTTCCTC	AGATGGGAATGGTTAAAGTG
NOTCH1	ATCTGAAATAGGAAACAAGTGAA	ATAACCAACGAACAACTACATAA
NOTCH2	AACATCTCATCCATGCTTTG	ACAGTGGTACAGGTACTTC
NOTCH4	ATTGACACCCAGCTTCTTG	GAGGACAAGGGTCTTCAA
OCLN	TTCTGGATCTCTATATGGTTCA	CCACAACACAGTAGTGATAC
P21	CTCTACATCTTCTGCCTTAGT	TCTCATTCAACCGCCTAG
PLVAP	CAATGCAGAGATCAATTCAAGG	ACGCTTTCCTTATCCTTAGTG
RARα	CCATCCTCAGAACTCACAA	ACCAGCGAGAATTAATACCT
RARβ	CACCTAGAGGATAAGCACTT	GGACTCACTGACAGAACA
RARγ	CCACCTTCTTGCTCCTAC	CTTTCACCCTCTGTTCCT
SLC2A1	ACGCTCTGATCCCTCTCAGT	GCAGTACACACCGATGATGAAG
SLC3A2	TTGGCTCCAAGGAAGATT	GAGTAAGGTCCAGAATGACA
SLC6A8	TGAGAGAATGAGATTTCTGCTTGT	TAGGGCTCACAGGGATGG
SLC6A12	AAGGTGGTTTATTTCACAGC	TTCAAGTAGTAGATGATGCCC
SLC7A1	CCTCCTGAGACATCTTTG	CTGGAATATGACGGGAAG
SLC7A5	TTGACACCACTAAGATGAT	GTAGCAATGAGGTTCCAA
SLC16A1	ACACAAAGCCAATAAGAC	ACAGAATCCAACATAGGTA
SLC44A5	TTTCTCCAGAGATGTTTCCC	TACAACACTTCTTGTCCCTC
STRA6	TTTGGAATCGTGCTCTCCG	AAGGTGAGTAAGCAGGACAAG
TLE1	TATTCCAGTCCAAAGAGTCC	AGATGACTTCATAGACTGTAGC
TFRC	ATGCTGACAATAACACAA	CCAAGTAGCCAATCATAA
VEGFR2	GTACATAGTTGTCGTTGTAGG	TCAATCCCCACATTTAGTTC
VWF	TGTATCTAGAAACTGAGGCTG	CCTTCTTGGGTCATAAAGTC
WIF1	AGTTGTTCAAGTTGGTTTCC	TAGCATTTTGAGGTGTTTGG
ZO1	CCTGAACCAGTATCTGATAA	AATCTTCTCACTCCTTCTG
βACTN	CGTCTTCCCCTCCATCGT	GATGGGGTACTTCAGGGTGA

Table S3 - Details of antibodies used for immunofluorescence and flow cytometry. Related to all main Figures and Supplemental figures.

Antibody	Dilution	Technique	Supplier	Catalog Number
CD31	1:50	ICC	DAKO/Labometer	M0823
VE-CADHERIN	1:100	ICC	Life Technology	sc-9989
TIE-2	1:100	ICC	R&D Systems	AF313
vWF	1:100	ICC	Dako	A0082
ZO-1	1:200	ICC	Life Technology	61-7300
CLAUDIN-5	1:100	ICC/Flow cytometry	Life Technology	34-1600
OCCLUDIN	1:200	ICC/Flow cytometry	Life Technology	71-1500
GLUT-1	1:50	ICC/Flow cytometry	Millipore	07-1401
PGP	1:10	ICC	GeneTex	GTX23364
ICAM-1	1:100	Flow cytometry	Santa Cruz Biotechnology	sc-107
*PE-conjugated anti-VEGFR2	10:200	Flow cytometry	R&D Systems	FAB357P
*FITC-conjugated anti-CD31	5:200	Flow cytometry	EBioscience	11-0319-42
*PE-conjugated anti-PGP	5:200	Flow cytometry	Abcam	Ab93590
*FITC-conjugated anti-PGP	20:200	Flow cytometry	BD Pharmigen	557002
*PE-conjugated anti ICAM-2	5:100	Flow cytometry	BioLegend	328506
R-PE conjugation KIT		Flow cytometry	Abcam	Ab102918
Phalloidin-fluorescein	50 µg/mL	ICC	Sigma	P5282
Anti rabbit Cy3	1:100	ICC/Flow cytometry	JacksonImmuniResearch	111-165-144
Anti mouse Cy3	1:100	ICC/Flow cytometry	Sigma	C2181
Anti rabbit Alexa 488	1:200	ICC	Life Technology	A11034
Anti mouse Alexa 488	1:200	ICC	Life Technology	A11001
Anti mouse Alexa 555	1:200	ICC	Life Technology	A21422

Table S4 - Details of products used. Related to experimental procedures.

Product	Supplier	Catalog number
EGM-2 bullet kit	Lonza	CABRCC-3162
FGF-b	Peprotech	167100-18B-B
BMP 4	Peprotech	120-05ET
VEGF	Peprotech	100-20
Tβ4	Caslo peptide synthesis	S-1298
Wnt3a	R&D Systems	5036-WN
SB 431542	Tocris	1614
RA	Sigma	R2625
Transferrin	Sigma	T8158
Insulin	Sigma	I9278
TNF-α	Peprotech	300-01A
CD31 MACS beads	Miltenyi Biotec	130-102-608
Lucifer yellow	Sigma	L-0259
Sirius red/fast green collagen staining kit	Chondrex	9046
Blyscan glycosaminoglycan kit	Biocolor	054B1000
Matrigel	BD	354234
Fibronectin	Calbiochem	341631